Université Abdou Moumouni

Doctoral Research Program on

Climate Change and Energy

(DRP-CCE)

Niger

SPONSORED BY THE

INTERNATIONAL MASTER PROGRAM

IN RENEWABLE ENERGY AND GREEN HYDROGEN (IMP-EGH)

SPECIALITY: PHOTOVOLTAICS AND GREEN HYDROGEN TECHNOLOGIES

MASTER THESIS

Topic:

METALLIZATION OF SILICON HETEROJUNCTION SOLAR CELLS BY COPPER PASTE DISPENSING

by:

Issifi Yacouba Mohamed

Panel members:

Chairman: Pr Modou Fall (Faculty of Science and Techniques, University of Check Anta Diop, Dakar, Senegal)

Examiner: Dr Hassan Adamou (Faculty of Science and Techniques, Abdou Moumouni University of Niamey, Niger)

Supervisors:

Prof. Dr. Rabani Adamou (Faculty of Science and Techniques, Abdou Moumouni University of Niamey, Niger)

Dr. Souley Kallo Moutari (École Normale Supérieure, Abdou Moumouni University of Niamey, Niger)

Prof. Dr. Uwe Rau (Director of Institute for Energy and Climate Research, IEK-5 at Forschungszentrum Jülich)

Dr. Kaining Ding (Head of Silicon Heterojunction Solar Cells and Module Department at IEK-5)

Academic year 2023-2024

DEDICATION

I dedicate this master's thesis to the people who have been my pillars of strength, unwavering support, and source of inspiration throughout this journey. Particularly:

To the memory of my beloved father Issifi Yacouba. Although he is no longer with us, his unwavering, endless encouragement and unyielding support continue to inspire me every day. and my beloved mother for her patience, belief in my abilities, and unyielding support continue to inspire me every day.

To all my family, whose boundless love and encouragement have fueled my pursuit of knowledge. Your belief in me has been the driving force behind every step I've taken.

To my friends, for the shared laughter, moments of respite, and camaraderie that have made the challenges bearable and the successes sweeter.

To the countless teachers, colleagues, and mentors who have crossed my path, thank you for your wisdom, guidance, and the invaluable lessons you've imparted

And finally, to all those who believe in the power of education and the pursuit of knowledge, this work stands as a testament to your unwavering faith in my potential.

This thesis is a reflection of your collective support, and it is with immense gratitude that I dedicate it to you.

ACKNOWLEDGEMENTS

All the praises and thanks be to Allah, the almighty for giving me health, patience, time, and strength to finish this work.

I am deeply grateful and honored to have reached this milestone, and I owe my heartfelt appreciation to the many individuals who have contributed to the completion of this master's thesis.

First and foremost, I would like to express my sincere gratitude to my thesis advisor Dr. Andreas Lambertz, Pr. Rabani Adamou, Dr. Souley Kallo Moutari, Dr. Kaining Ding, and Mr. Yanxin Liu for their invaluable guidance, unwavering support, and insightful feedback. Their expertise and encouragement have been instrumental in shaping the direction of this research.

My sincere appreciation goes to the Federal Ministry of Education and Research (BMBF) and the West African Science Center on Climate Change and Adapted Land Use (WASCAL) for providing the scholarship and support for this program.

Special thanks to Pr. UWE Rau and all the IEK-5 staff, and Forschungszentrum Jülich GmbH (FZJ) at large, for their hospitality, support, assistance, and words of encouragement to accomplish this research.

Many thanks to Prof. ADAMOU Rabani (Director of WASCAL DRP CCE), Ass. Prof. INOUSSA Maman Maarouhi (Coordinator and Deputy Director of Wascal DRP-CCE) Ass. Prof. MOUNKAILA SALEY Moussa (Scientific Coordinator Wascal DRP-CCE), Dr. AYOUBA MAHAMANE Abdoulkadri (Coordinator IMP-EGH Program, Wascal DRP-CCE), and all the staff of WASCAL DRP-CCE for their hard work and deep implication in the successfulness of this program.

I would like to thank the dean Faculty of Science and Techniques (University of Abdou Moumouni) for providing the resources and environment essential for conducting this program. The libraries, laboratories, and facilities have played a crucial role in my academic pursuits.

I am deeply thankful to my friends, colleagues, and fellow students who provided moral support, words of encouragement, a shoulder to lean on during moments of stress, and shared experience, enriching my understanding of the subject matter. Your camaraderie has made this journey all the more rewarding.

My sincere appreciation goes to my family for their unwavering support, patience, and belief in my abilities. Your love and encouragement have been my pillars of strength.

While it is impossible to mention everyone by name, please know that your contributions, whether big or small, have not gone unnoticed and are deeply appreciated.

Thank you all for being an integral part of this journey.

Abstract:

In terms of global photovoltaic (PV) manufacturing capacity, crystalline silicon (c-Si)-based technologies account currently for 95% of the market, and one the most efficient technologies, among them, is the silicon heterojunction (SHJ) solar cell technology (efficiency above 26%). Nonetheless, this silicon-based photovoltaic is experiencing a threat due to the increasing price of silver, which is influenced by its shortage. For SHJ solar cells, silver usage for metallization accounts for approximately 25% of the total solar cell processing cost due to its large silver consumption. The findings emphasize that dispensed copper is a great alternative to silver for SHJ solar cell application, and it has a strong potential to reduce costs and improve cell efficiency. However, there are still obstacles to address for this technology. On one hand, dispenser printing technology needs to be improved in terms of printing quality, and on the other hand, copper reliability in terms of adhesion and electrical performance needs to be addressed. This research focuses on studying the characteristics of a single print dispensing, the process conditions of dispensed copper, the effect of those conditions applied to SHJ solar cells, and lastly the performance study of SHJ solar cells metalized with dispensed copper, then their comparison to other printing technology such as screen printing. It was found that dispensed Cu still has higher line resistance to screen-printed silver and that SHJ solar cells degrade above 280℃ and 5 s sintering conditions, though we could partly recover some loss with light soaking. SHJ solar cells metalized with dispensed Cu achieved an efficiency of>23% and a V_{oc} of about 740 mV. This study advances SHJ solar cell technology by providing insights into the future potential of using dispensed copper metallization for improved and cost-effective solar cells.

Keywords: **Silicon heterojunction solar cell, metallization, silver consumption, dispensed copper, screen printing.**

Résumé :

En termes de capacité de production photovoltaïque (PV) mondiale, les technologies basées sur le silicium cristallin (c-Si) représentent actuellement 95 % du marché, et l'une des technologies les plus efficaces est la technologie des cellules solaires à hétérojonction de silicium (SHJ) (efficacité supérieure à 26 %). Néanmoins, cette technologie photovoltaïque à base de silicium est menacée par l'augmentation du prix de l'argent, qui est influencé par sa pénurie. Pour les cellules solaires SHJ, l'argent utilisé pour la métallisation représente environ 25 % du coût total de traitement des cellules solaires en raison de sa forte consommation d'argent. Les résultats soulignent que le cuivre distribué est une excellente alternative à l'argent pour les applications de cellules solaires SHJ, et qu'il a un fort potentiel de réduction des coûts et d'amélioration de l'efficacité des cellules. Toutefois, il reste des obstacles à surmonter pour cette technologie. D'une part, la technologie d'impression du distributeur doit être améliorée en termes de qualité d'impression, et d'autre part, la fiabilité du cuivre en termes d'adhérence et de performance électrique doit être examinée. Cette recherche se concentre sur l'étude des caractéristiques d'une impression unique, les conditions de traitement du cuivre dispensé, l'effet de ces conditions appliquées aux cellules solaires SHJ, et enfin l'étude de la performance des cellules solaires SHJ métallisées avec du cuivre distribué, puis leur comparaison avec d'autres technologies d'impression telles que la sérigraphie. Il a été constaté que le Cu distribué a toujours une résistance de ligne plus élevée que l'argent sérigraphié et que les cellules solaires SHJ se dégradent au-dessus de 280℃ et des conditions de frittage de 5s, bien que nous puissions partiellement récupérer une partie de la perte avec un trempage à la lumière. Les cellules solaires SHJ métallisées avec du Cu distribué ont atteint un rendement supérieur 23% et un V_{oc} d'environ 740 mV. Cette étude fait progresser la technologie des cellules solaires SHJ en donnant un aperçu du potentiel futur de l'utilisation de la métallisation au cuivre dispensé pour des cellules solaires améliorées et rentables.

Mots-clés : **Cellule solaire à hétérojonction en silicium, métallisation, consommation d'argent, cuivre distribué, sérigraphie**.

ACRONYMS AND ABBREVIATIONS

AM 1.5: air mass 1.5

Ag: silver

a-Si :H : hydrogenated amorphous silicon

CO_2: carbon dioxide

Cu : Copper

CCD : charge-coupled device

CSEM : swisse center for electronics and microtechnology

EQE : external quantum efficiency

EL: electroluminescence

eV: electron volt

FF: fill factor

FS: flat Surface

g: gramme

$GtCO_2$: gigatonne of CO_2

GWp : gigawatt peal

HJT: hetero Junction

IPCC: intergovernmental panel on climate change

ITO: indium tin oxide

IQE: internal quantum efficiency

ITRPV: international technology roadmap for photovoltaic

IWO: indium tungsten oxide

J_{sc}: Short circuit current density

J_{mpp}: maximum power point current density

Kg: kilogram

kW: kilowatt

LED: light emitting diode

mL: milliliter

mA: milliampere

μm: micrometer

nm: nanometer

Pa: Pascal

PERC: passivated emitted and rear contact

PECVD: plasma-enhanced chemical vapor deposition

PVD: physical vapor deposition

Pin: input power

Pmpp: maximum power point power

pFF: pseudo fill factor

PV: photovoltaic

RPM: revolutions per minute

Rs: series resistance

s: second

SHJ: silicon hetero junction

SP: screen printing

SMU: source measure unit

SE: step edge

TCO: transparent conductive oxide

TWp: terawatt peak

USD: united states dollar

V_{mpp}: maximum power point voltage

V_{oc}: open circuit voltage

W: watt

Wp: watt peak

¢: cent

Ƞ: efficiency

LIST OF TABLES

LIST OF FIGURES

Table of contents

Introduction

According to the Intergovernmental Panel on Climate Change (IPCC), if the 1.5°C limit is exceeded, climate change risks causing much more frequent and severe droughts, heatwaves, and heavy rains [1]. Since then, the Paris Agreement, which aims to "keep the increase in global average temperature to below 2°C above pre-industrial levels" and pursues measures "to limit the temperature increase to 1.5°C above pre-industrial levels," has received increased attention [2]. As reported by the IPCC, CO_2 emissions from fossil fuels are the primary driver of global warming. In 2018, fossil fuels and industry accounted for 89% of worldwide CO_2 emissions[3].

To attain the Paris Agreement objective, immediate and drastic reductions in CO_2 emissions across all sectors are essential by 2030. One of the most important approaches to reducing CO_2 emissions is the transition in the energy sector. Consequently, this will necessitate a significant reduction in the use of fossil fuels, improved energy efficiency, and the use of renewable energy, since it is a clean source of energy. For that, it is necessary to scale up all renewable power generation capacity across all regions. Additionally, in most locations, renewable energy sources are already the least expensive form of electricity.

Of all renewable energy resources, photovoltaics is one of the most prominent, due to its enormous advantages such as its abundance, cost-competitiveness, and its availability[4]. Along with wind power and hydropower, it is the most significant renewable resource and will dominate the growth of renewables in the electricity sector [5]. The IPCC Special Report on Carbon Dioxide Capture and Storage through some scenarios reported that the global annual CO_2 emissions could range from 29.3 to 44.2 $GtCO_2$ in 2020 and from 22.5 to 83.7 $GtCO_2$ in 2050[6]. However, photovoltaics (PV) can significantly reduce worldwide greenhouse gas emissions by 4 to 5 GWp CO_2 equivalent per year and therefore 40 to 50 GWp in ten years [7]. Breyer *et al* reported that, in the overall energy demand, the share of PV can be 36% to 42% globally [8].

Figure 1-1 shows that over recent years photovoltaic technology has demonstrated a successful development resulting in a cumulative capacity of 1 TWp [9]. Pierre Verlinden *et al.,* 2020 depicts the future potential demand for PV output, with 10 TWp of PV by 2030 and 30 to 70 TWp by 2050, which requires an annual PV production of 3-4 TWp per year by 2050.

The growth of the PV sector and large-scale production, especially in China, has led to a decline in the manufacturing cost of PV panels. Some improvements, such as an increase in silicon wafer size (from 100 mm to 210 mm), a reduction in wafer thickness (down to about

150 µm), a reduction in silver consumption (from 50 mg.Wp^{-1} to less than 19 mg.Wp^{-1}), automation, and an increase in throughput per tool, are cited as reasons for this manufacturing cost reduction [9].

However, there are obstacles to this pace of expansion. It is worth noting that, despite reaching grid parity in many regions of the world, yearly growth in the PV market has slowed since 2018 to around 10% to 11% p.a. Therefore, it will be difficult to achieve a total installed capacity of 70 TWp by 2050 with this rate of annual growth, and the world will be obliged to speed up the deployment of PV technology in the final few years before 2050 to meet the goal of zero CO_2 emissions. According to Pierre Verlinden *et al.*, 2020 Fast growth in PV production capacity (25% to 30%) is projected until 2032 [see **Figure 1-1**], after which it will settle at roughly 3TWp yearly from 2032 to 2055 [9].

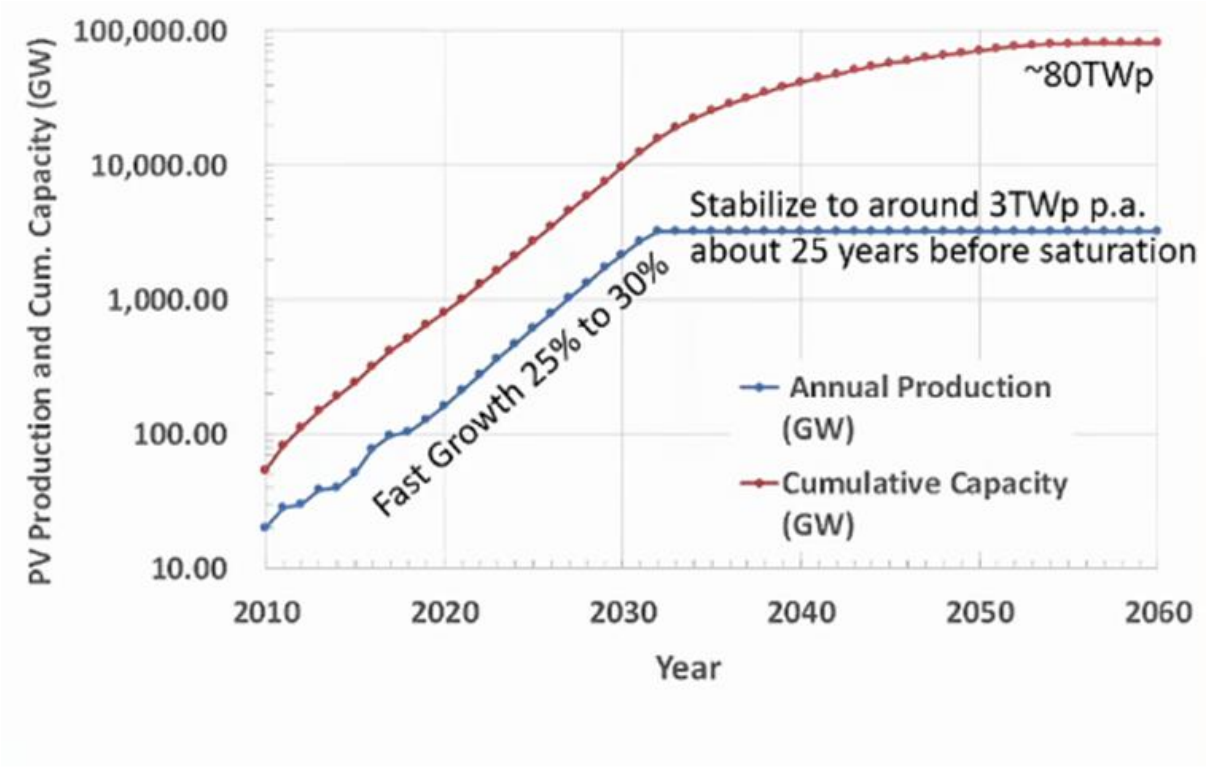

Figure 0-1: Growth of PV production and cumulative capacity versus year [9].

One of the most important obstacles, particularly for beyond terawatt per year production capacity, is the unavailability of some materials, such as silver for metallization [9]. The metallization is critical in producing high-efficiency, low-cost crystalline silicon solar cells as the metal contacts have to extract and transport photogenerated charge carriers, with low resistance. The amount of silver used per cell has dropped and is expected to decrease in the

next years. Nevertheless, a certain minimum conductivity is required by the metallization [10]. The metallization of the solar cell includes the fingers and busbars. The Fingers are line conductors that extract and transport photogenerated charge carriers to the busbars which are electrically connected to the ribbons or wires for interconnection of the solar cells in the solar module [11]. The electrical contact resistance between the metal fingers and semiconductor has to be small and for heterojunction solar cells the electrical contact between the transparent conductive oxide (TCO) and the fingers is relevant [12]. Another important issue about the metal fingers is that it is highly required to make them narrow, to reduce the shading loss of the incident sunlight.

On average, an industrially produced 21% efficient PERC solar cell in 2020 utilized 90-100 mg of silver when using 166 ×166 mm^2 silicon wafers, corresponding to a silver usage of approximately 15.4 $mg.Wp^{-1}$ [13]. The PV industry today utilizes approximately 20 tons of silver per GWp (2400 tons of silver in 2019), accounting for slightly more than 10% of the global silver consumption [16]. The current cost of silver paste is estimated to be USD 820/kg for high-temperature paste and USD 1060/kg for low-temperature paste [10]. Five busbars and a bifacial SHJ solar cell (23%, 5.62W, M2 wafer) require around 350 mg of low-temperature silver paste. Based on the current silver paste price the cell costs around 35 cents each [14]. Additionally, Louwen *et al.,*2016 reported that the overall metallization cost is 0.55 USD per wafer or 0.10 USD per Wp [10]. Considering the previous information, if nothing changes in the PV sector's usage of Ag per Wp, the PV industry will consume 100% of global silver production at 1 TWp per year production (about 2028). To achieve material sustainability, the PV sector will need to cut Ag usage to less than 5 $mg.Wp^{-1}$, for example, by substituting silver with copper [8]. This means that if Ag consumption does not decrease in the next few years, this will not only lead to more expensive solar cells but will also hinder the future growth of the PV industry [15].

Among the silicon-based PV technologies, the SHJ solar cell is attracting more attention due to its high efficiency, excellent passivation, low-temperature process, and simple design [16]. Longi revealed that the SHJ solar cell efficiency has been steadily increasing in recent years, reaching an efficiency of 26.81% [17] for two sides contacted structures and Sanyo developed the SHJ concept, which was first introduced in 1990 [18]. Silicon heterojunction solar cell is particularly appreciated because it constitutes a solution for the main problem that is preventing silicon solar cell from achieving the theoretical efficiency of 29.4%. The problem is due to the recombination of the generated carriers at the metallic electrical contacts. The

excellent hydrogenated amorphous silicon surface passivation layer helps to reduce significant carrier recombination. Its low-temperature process implies using low-temperature silver and a greater amount of silver paste for a highly conductive metallization which dramatically affects the cost of SHJ solar cells. Thus, for SHJ solar cells, lower silver paste usage or the substitution of expensive silver paste is in great demand [14]. The below figure (**Figure 0-2)** shows us the schematic drawing of SHJ solar cell at IEK-5 with all the details.

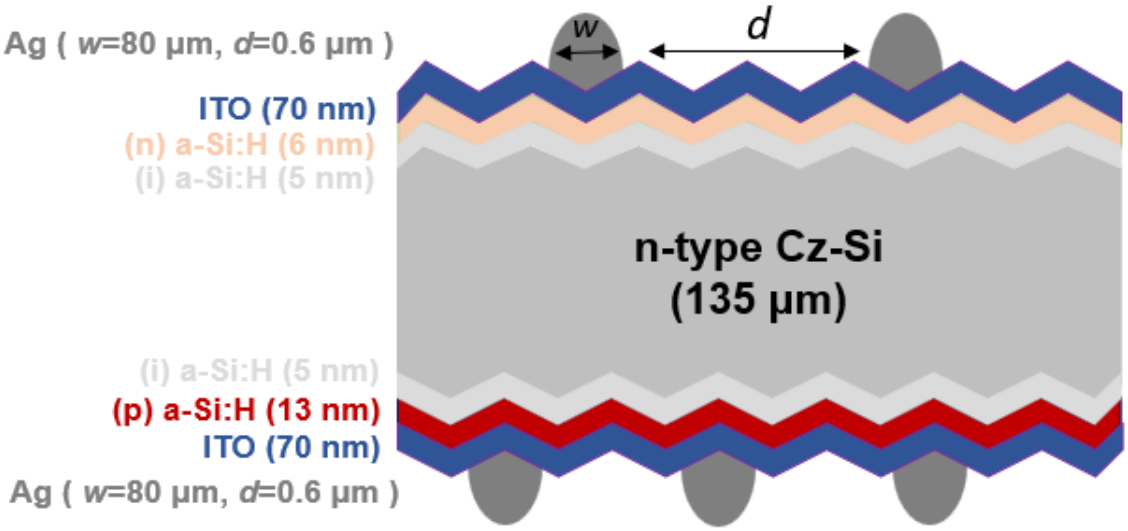

Figure 0-3: Schematic drawing of the band diagram of a SHJ solar cell at IEK-5

To further reduce the silver consumption in solar cells, according to [19], researchers are proposing different paths:

- fine-line screen printing (SP): this consists of printing fine lines with traditional screen printing and enhancing the aspect ratio without compromising the cell's efficiency. in agreement with, it has been demonstrated that, despite the typical challenges with the use of the SP regarding the materials (screen, paste), by using a knotless screen ultra-thin contacts could be achieved with an average finger width of less than 20 µm (without busbars) with a maximum efficiency up to 22.83% [20].
- fine line printing with other technologies: some of the ways to reduce silver consumption while printing is, to use newly developed appliances such as laser pattern transfer printing, rotary screen printing, flex trail-printing, and dispenser printing with a very low silver consumption capacity, and high aspect ratio for fine line metallization. dispenser technology is prominent for this purpose and helps to achieve up to below 17

μm according to pospischil *et al.*, 2019 on a PERC solar cell. furthermore, they demonstrated in that study that the ag laydown along with electrical cell performance was enhanced over the reference [21], [22].

- reduce or replace silver with copper: because copper is more abundant (1000 times), cheaper (100 times), and more eco-friendly than silver, it constitutes a prominent alternative for silver, although it is less conductive (about 5%) and less resistant to oxidation than silver [23]. moreover, cu has a proven track record in microelectronics because of its low resistivity and good electromigration resistance and is widely used as an interconnect in ultra-large-scale integrated circuits. in this regard, cu could be a suitable metal for the metallization of solar cells [24]. copper plating has already been used for many years and resulted in a very high efficiency on heterojunction solar cells according to SunPower [25] and SunDrive even recorded recently 26.1% efficiency on a full-size silicon heterojunction (HJT) solar cell featuring its copper-based technology [26]. in the same way, to reduce silver consumption another exciting alternative could be silver-coated copper, particularly on heterojunction devices or using copper paste as busbars [19]. copprint has already made a high-conductive and low-cost copper nano ink for solar cell metallization that can help to save cost for up to 70% relative to top silver pastes due to its high conductivity and of course, could significantly reduce the heterojunction solar cell production cost [27] but its compatibility to SHJ solar cells has to be shown. apart from the abundance and low cost of copper, SunDrive discovered that we can enhance efficiency above and beyond what silver can achieve [26].

This research will investigate the performance of copper as metallization on silicon heterojunction solar cells using dispenser printing, which will contribute in the sense of reducing silver consumption, hence reducing the production cost of solar cells. And particularly, it will evaluate how to find the proper copper finger handling conditions to achieve high performance in SHJ solar cells and how to use a single print dispenser.

1) Problem statement

According to P.J. Verlinden *et al.,*2020 by 2050 an overall implementation of about 70 Terawatts of PV is planned to be achieved, as revealed by many studies. This implies a required production of 3-5 TWp annually, in 2035-2050, of PV panels. However, to meet this target, some challenges need to be addressed. One of the most critical ones is the shortage of silver, which is currently used as a principal metal paste for silicon metallization. And this silver shortage, obviously will lead to an increase in its price. The PV industry, currently, uses more than 10% of the global silver production [9], also 10% of the PV module costs are covered by silver [28] and according to the international technology roadmap for photovoltaic ITRPV 2023, SHJ devices consume even higher [29]. Recently, its share in module cost has increased to 5%[28] and it is expected to grow [30] as shown in **Figure 1-3**. Some ways were proposed to address this challenge such as reducing the silver consumption to less than 5 mg.Wp^{-1} [9] or even less than 2 mg.Wp^{-1} [13]. If this problem is not solved, solar module prices will continue to rise, which in turn will threaten the growth of the PV industry. To achieve the latter goal, replacing silver with copper is a great option. Though, copper in turn also possesses many drawbacks such as its lower performance and lesser resistance to oxidation compared to silver [23]. Additionally, technology for achieving very thin finger width and high aspect ratio is enormously critical, to reduce the shading loss of the cells.

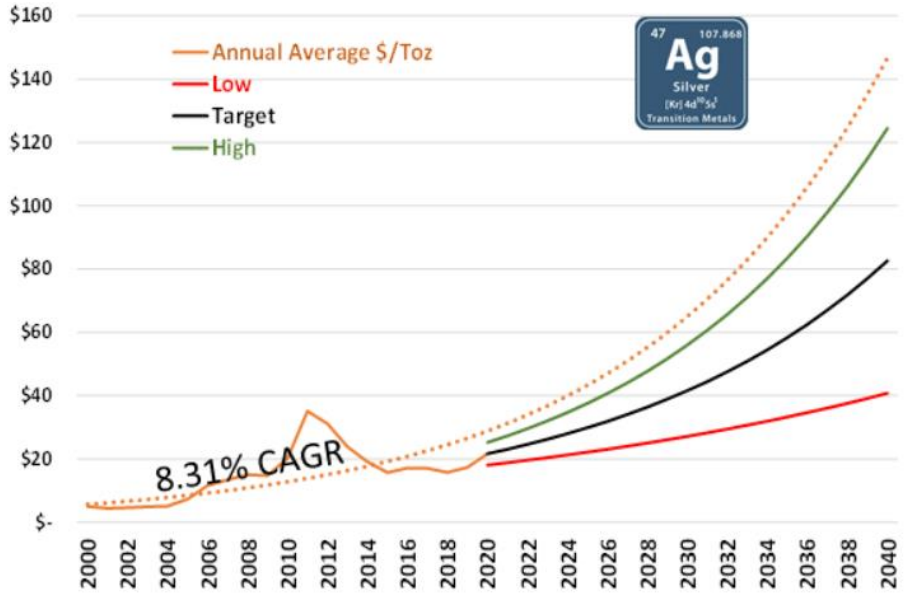

Figure 0-4: The long-term silver price forecast over the years until 2040 based on four different trends: the annual average, the low average, the target average, and the high average of the long-term silver price forecast [30].

2) Research questions

- Can copper paste replace efficiently silver paste as metallization on high-efficiency silicon heterojunction solar cells?
- What is the suitable process/treatment condition for copper as metallization on silicon heterojunction to reach good performance?
- Is dispenser printing a convenient way for metallization and could it replace the usual screen printing?
- Can SHJ solar cells withstand the Cu process conditions and is it possible to recover the SHJ performance solar cell after curing?

3) Research hypothesis

Using dispensed copper paste as metallization for silicon heterojunction solar cells reduces silver consumption and production costs, while dispenser printing enables low width, high aspect ratio finger lines to enhance solar cell efficiency.

4) Research objectives

a) Main objective

- Investigate the performance of SHJ solar cells metalized with dispensed copper.

b) Specific objectives

- Understanding how dispenser printing functions and operates
- Investigating the best process conditions for utilizing copper paste on silicon heterojunction solar cells
- Fabricating and evaluating the performance of SHJ solar cells metalized with dispensed Cu.
- Investigation if the SHJ solar can withstand the process conditions used for the curing of the copper paste.

5) Research outline

There are six chapters. The first is the introduction, and the literature review is presented in the second chapter. The third chapter will be devoted to methods and techniques. The experimental work and results of this research are fully described in chapter 4, then discussions and interpretations of results are given in chapter 5. Chapter 6 is conclusion and outlook for the follow-up of this study.

Chapter1: Literature review

Silver paste has been traditionally and widely used as material for metallization, because of its good electrical conductivity and good contacts for silicon solar cells in general. The metallization of silicon heterojunction solar cells is one of the key steps in its fabrication process, defining the electrical contact and largely the performance of the device. However, this material possesses some challenges that need to be addressed such as its scarcity which is leading to its increasing price. Hence, to sustain the growth of PV production, there is an urgent need to explore alternative metallization materials to address those challenges. Copper is a prominent candidate, because of its cost-saving potential and improved electrical performance.

This section consists of an overview of the research done in the field of dispensed copper metallization on SHJ solar cells, stressing the advances accomplished and some remaining problems.

1) Metallization of silicon heterojunction solar cells

Metallization is one of the most critical steps in the process of fabrication of silicon solar cells. It provides electrical conductors on the surfaces of solar cells to collect photo-generated charge carriers [11]. When light with an energy above the bandgap of the semiconductor (Si), charge carriers are photogenerated. They are separated by the selective contacts and it is where the role of metal contact starts. The promoted charges carriers are being conducted by the metal contacts, precisely the fingers and those fingers transport those carriers to the busbars, which in turn will transfer the electricity out of the solar cell (see **Figure 2-1**). It (fingers and busbars) allows interconnecting cells by ribbons to a string and the strings are further interconnected to form a module, capable of operating a load [31].

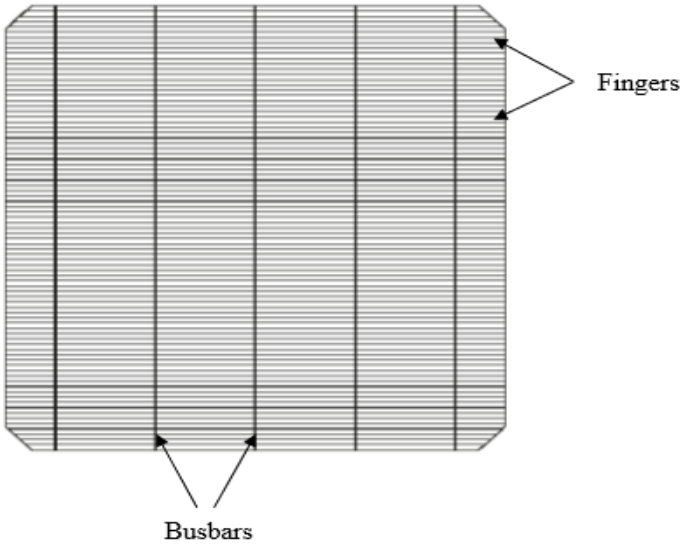

Figure 1-1: Front-side metal contact design in a solar cell

This **figure 2-1** shows the front-side metallization principle of a solar cell. For standard silicon heterojunction solar cells at IEK-5, on the front side are 96 fingers screen-printed with a width of 45 µm in a double print process to ensure a small width with enough height. On the backside, 250 fingers are screen-printed with a width of 60 µm. Afterward, the paste is dried and the solar cells are annealed for 40 min at 170°C [32],[33]. The width of the fingers is crucial, particularly for the front side of solar cells. Since the fingers are not transparent to light, they lead to shading losses. The optimization of the finger number and consequently the distance between fingers (pitch), plays a big role in reducing or increasing shading losses and ohmic losses [11]. An increase in the aspect ratio (height to width) of the fingers reduces the finger resistance resulting in an improvement in the solar cell's efficiency. Routes to increase the solar cell efficiency are: firstly, increasing the fill factor by reducing the finger resistance, and the contact resistance, and increasing the aspect ratio. Secondly, we have to enhance the short circuit current density, mainly by reducing the finger width, therefore reducing shading loss [24]. The latter is related to the percentage of the area for the metallization [11].

The outstanding performance of the silicon hetero-junction (SHJ) solar cells due to the hydrogenated amorphous silicon a-Si: H surface passivation made this device an attractive choice for cost-effective high-efficiency solar cells. Its production contains a few steps: the wafers are textured by alkaline wet chemical etching, followed by wet chemical cleaning. Subsequently, in a plasma-enhanced chemical vapor deposition (PECVD) process, a few manometers of intrinsic and doped a-Si: H layers are deposited on both sides of the Si wafer, generating an a-Si: H i-n stack on the front side and a-S i: H i-p stack on the rear side. Then sputtering the TCO at the front and back with varied thicknesses, and finally printed the metal contact (**Figure 2-2**) [33].

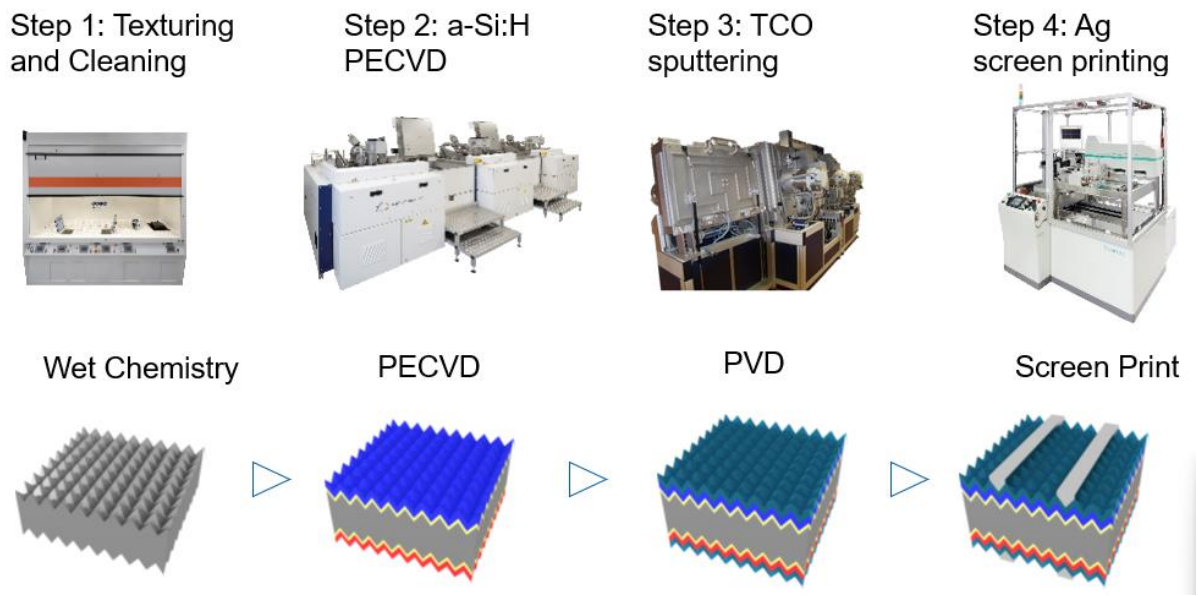

Figure 1-2: Fabrication process of SHJ solar cell at IEK-5

Since SHJ solar cells are sensitive to temperatures above 200°C, its metallization has to be conducted at low temperatures with pastes (silver, copper...) suitable for temperatures <200°C, as opposed to passivated emitter for rear contact PERC devices, where silver pastes are fired at temperatures around 800℃. The disadvantage is that low-temperature pastes are more expensive than conventional PERC paste [16].

According to the National Renewable Energy Lab, it is estimated that the metallization cost is around 4 ¢/Wp as opposed to 1.69 ¢/Wp for PERC [16], the international technology roadmap for photovoltaic (ITRPV) as shown in **Figure 2-3** confirmed that SHJ solar cells are the most consuming, due to the use of silver in front and entire rear side. This figure projects that silver (Ag) consumption will be significantly reduced. However, this requires more effort and development for the narrow line printing technologies such as dispenser printing, laser transfer printing… etc., which allow finger width below 29 µm. Silver replacement is also considered, for instance by copper [29].

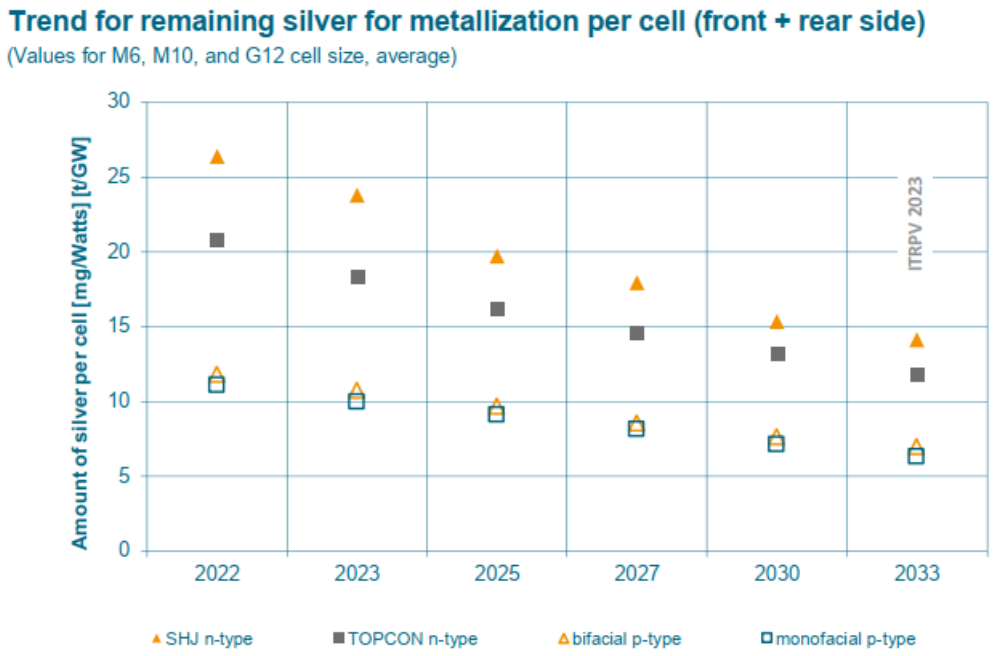

Figure 1-3: Trend for remaining silver per cell Wp for different cell concepts as average consumption for M6, M10, and G12 wafer formats [29].

One thing about SHJ solar cells is that the metal contacts that cause high recombination in conventional silicon solar cells are made on a transparent conductive oxide (TCOs), which is a conductive layer inserted on top of a stack of intrinsic and doped a-Si: H layers. Yu, Jian, *et al.*, 2021 reported that this TCO film has an excellent copper diffusion barrier [14], resulting in a high open-circuit voltage (V_{oc}) and fill factor (*FF)*. This copper metallization could be accomplished using many methods such as physical vapor deposition, screen printing, metal plating, and alternative printing techniques such as stencil printing, inject-printing, dispensing, transfer pad printing, and so on (see **Figure 2-4**) [10].

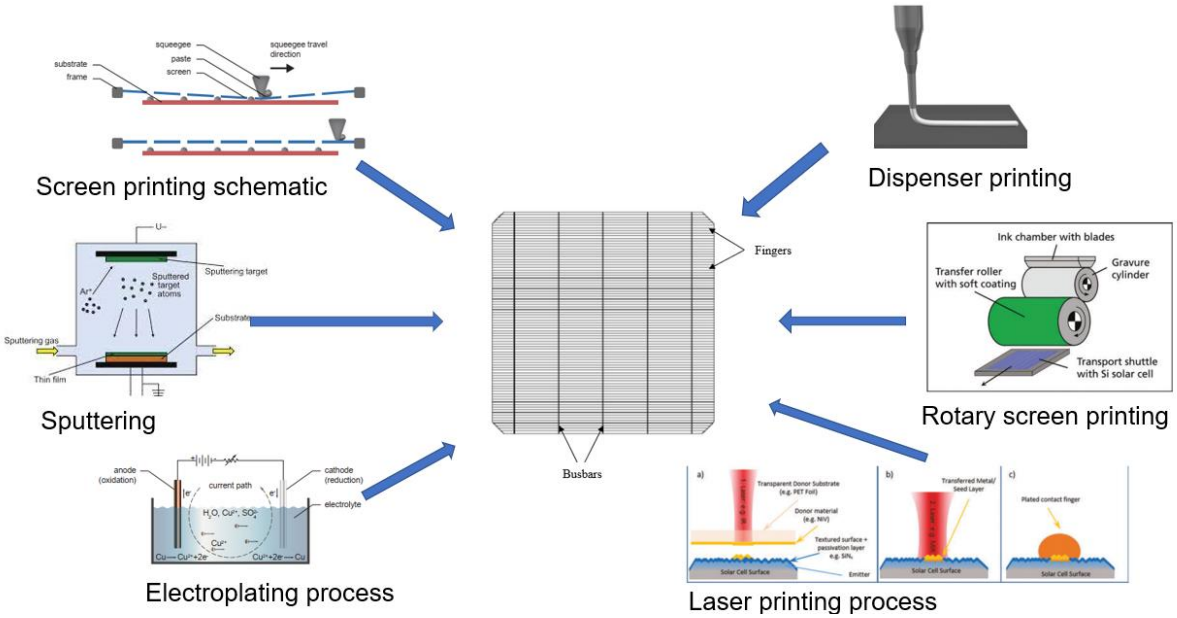

Figure 1-4: Metallization approaches for solar cells [11]

Currently, the standard metallization of solar cells is to print silver fingers by a screen-printer. The latter is the most widely used technology for this metallization because of its great cost efficiency, reliability, and less complexity [31] and gives great freedom for finger design [27]. However, the screen-printing technology has some limitations like finger interruption, excessive spreading, reduced lifetime, and higher cost of the knotless screen [21], alternative printing approaches were developed and adopted, which are more suitable for very thin fingers (width less than 20 µm) and require less paste. Furthermore, among those alternative printing methods, pressure-driven dispensing is regarded as promising due to its remarkable advantages of fine finger electrodes with high aspect ratio and homogeneity through a single print run without direct contact with the solar cell pad [34], particularly compared to screen printing, as seen in **Table 1**.

Table 1: Comparison of various metallization approaches based on: typical finger dimensions (the range includes front and rear metallization), typical specific contact resistivity (the range includes results on uniformly or selectively doped regions), availability of mass production tools ('+' for 5 tool vendors, '+++' for >10 tool vendors), typical throughput, typical tool and consumables costs ('+' for high cost, '+++' for low cost), and estimated market share [11].

Category	Sub-category	Typical finger width [µm]	Typical finger height [µm]	Typical aspect ratio (AR)	Typical specific contact resistivity [mΩ cm²]	Availability of mass production tools	Typical throughput [wph]	Typical tool costs	Typical consumables costs	Estimated market share [%]
PVD	Metals	–	–	–	0.01–2	+++	3 000–10 000	+	++	<3
	TCO	–	–	–	15–200	+++	3 000–10 000	+	++	<3
Screen printing of metal pastes	Mesh screens	30–80	20–40	0.25–0.67	0.1–10	+++	3 000–4 500	+++	++	>90
	Stencil	30–80	20–40	0.25–0.67	0.1–10	+++	3 000–4 500	+++	+	<2
Alternative printing of metals pastes or inks	Ink-jet of metals	30–80	1–5	0.03–0.1	0.1–10	+	3 000–4 500	++	+	<1
	Aerosol jet	30–80	5–10	0.1–0.2	0.1–10	+	3 000–4 500	++	+	<1
	Laser transfer	20–80	20–40	0.25–1.0	0.1–10	+	3 000–4 500	++	+	<1
	Dispensing	20–80	20–40	0.25–1.0	0.1–10	+	3 000–6 000	++	++	<1
	Rotary printing	30–80	10–20	0.13–0.25	0.1–10	+	5 000–10 000	++	++	<1
Plating	Directly on Si	15–40	5–20	0.13–0.50	0.1–2	++	3 000–4 500	+	+++	<1
	Seed-and-plate	15–40	15–40	0.25–1.0	0.1–2	++	3 000–4 500	+	++	<2

According to Erath D *et al*., it has already been reported achievement for the first time of dispensing a low-temperature silver paste, though finer line dispensing was found with the conventional high-temperature silver paste [35], [36].

1.1) Dispenser printing

For years, solar cell researchers have been working to develop a non-contact metallization technology that would reduce rejections during the printing process while also eliminating the need for crystal screen replacement [37]. Dispenser printing is a contactless printing process, with high throughput, and offers single-step metallization techniques, where a paste is extruded through a small nozzle opening which is moved relatively towards the substrate forming either dots or continuous lines [38]. This contactless approach (i.e., nozzle and substrate do not touch), offers the possibility to adapt paste rheology in a much wider range than other thick film printing technologies and permits to achieving of very thin finger width, with a high aspect ratio, and line homogenous compared to screen printing [11]. The flow rate of the paste is determined by the applied pressure, needle diameter, and needle length. Furthermore, the flow rate is greatly controlled by the paste's dynamic viscosity, which is influenced by the shear rate and temperature [39]. The throughput rate is an important economic aspect. It determines the number of cells that can be made per hour, therefore the higher it is, the lower the production cost per solar cell [11]. Dispensing metal grid line was demonstrated by Hanaoka in 1992 [16]. Nonetheless, due to the rapidly developing screen-printing

technology at the time, there was little interest in it. However, at Fraunhofer ISE, several researchers continued to work on developing it, to bring this technology to an industrial scale [22]. Recently, outstanding results for several cell designs using high-throughput parallel dispensing have been reported. For that, 10 to 50 nozzles were scaled to function in parallel [24,25]. This comprised the parallel dispensing of 150 Ag contacts with a finger width of only 17 µm for p-type PERC [22]. As reported by Gensowski *et al.*, 2022 for SHJ solar cell, using a nozzle opening 25 µm parallel dispensing showed a finger width of 34 µm and an increased aspect ratio of 0.55 [40]. For this technology to be suitable for the industrial metallization of solar cells, dispensing must be parallelized [37]. Moreover, the application of dispenser printing on solar cells, fine-line printed front contact has shown an absolute efficiency increase of about 1% compared to respective screen-printed references over the years and an efficiency increase of about 2 % relative to respective screen-printed contacts by GECKO project [37]. The absence of mesh marks reduced the silver (Ag) laydown by 20% without reducing grid conductivity with commercially available screen-printing pastes [25]. Additionally, it was demonstrated by stretching effect, with a nozzle of 30 µm opening further reduction of the Ag laydown from m_{ag}=0.84mg to m_{ag}=0.54mg per line electrode and that corresponds to an absolute decrease of δmag=32%abs [40],[41]. Considering these improvements, dispenser constitutes prominent option to achieve the ITRPV predictions for finger width (see **Figure 2-5**) [42]. Nevertheless, most of the remarkable contact geometries provided have not yet reached low-temperature paste which is necessary for SHJ solar cells [22]. Regardless of all, dispensing is still a developing technology and it requires much work to further address accompanying challenges.

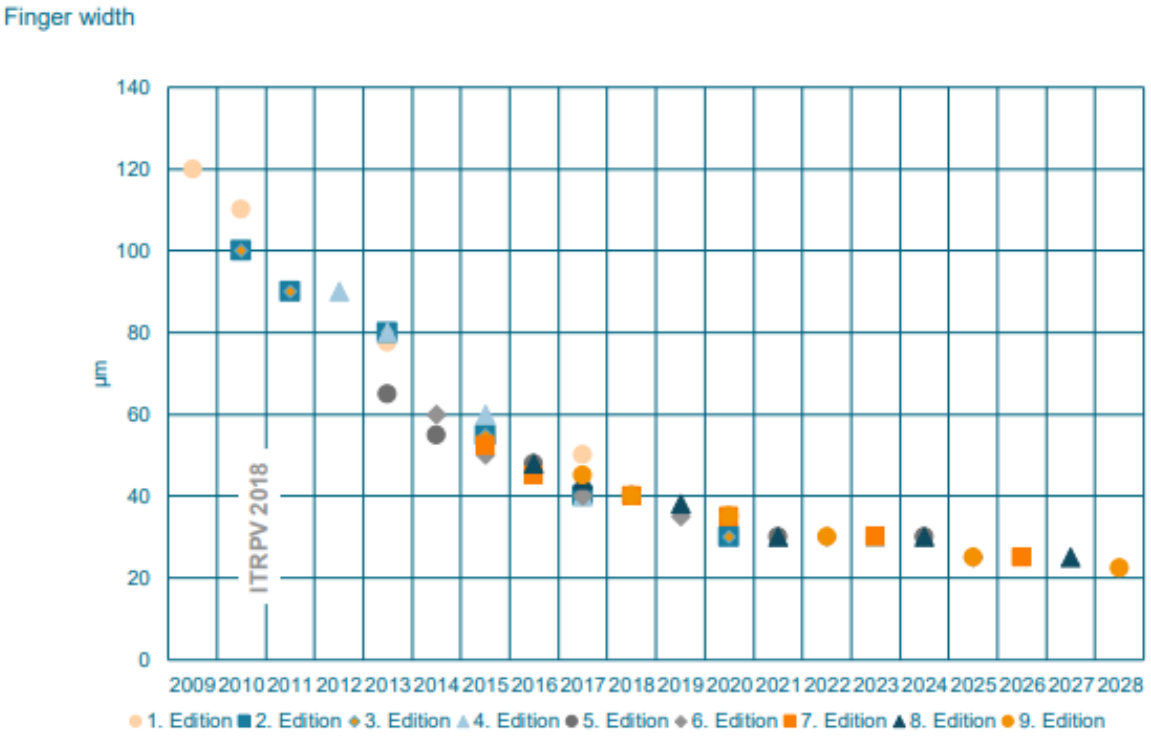

Figure 1-5: ITRPV predictions for finger width[42]

1.2) Copper metallization on SHJ solar cell

Silver is the traditional metal used for the metallization of SHJ solar cells, and silicon solar cells at large due to its tremendous advantages such as it has high electrical contact, low contact resistance, high oxidation resistance, excellent adhesion, long-term stability…etc. However, this silver is one the most critical and expensive non-silicon materials [43]. The price of silver paste is directly dependent on the volatile silver metal price [44], and that constitutes a threat to the growth of the PV industry and the rising cost of solar cells. Alternatively, copper is second only to silver in terms of conductivity and could replace silver for the metallization of SHJ solar cells. Additionally, copper is more abundant than silver (1000 times more abundant), cheaper than silver (100 times cheaper), and has less carbon footprint than silver (3.97 vs. 155 $kgCO_2/kg$ respectively), all good reasons to transfer to copper metallization (see **Table 2**) [44],[23]. Copper plating has already been explored for decades, which not only significantly reduces silver consumption, but offers tremendous advantages including better conductivity and great ability of finer fingers [45],[46]. Furthermore, silver-coated copper is another approach that has been developed in recent years. It is cost-effective and could give efficient solar cells [47].

Oxidation and diffusion are the main challenges when copper is metallization for solar cells [48]. Unlike previous generations of low-temperature Cu pastes, which were based on micron-sized Cu particles and required special measures to prevent Cu oxidation, such as low melting temperature alloy coating or annealing in an inert atmosphere, the new pastes are based on nanoparticles and can be processed more easily [48]. With regards to the Cabrera–Mott theory for oxidation of metals, metal electrons travel to the surface and react with adsorbed oxygen molecules, creating oxygen anions. Then, due to the surface dipole between the metal cations and the oxygen anions, metal oxides develop at the surface, it can be imagined possible to prevent copper oxidation by hindering electron release from metal atoms or blocking oxygen adsorption.

Endothermically, the way copper gets oxidized is that: when oxygen is adsorbed on the Cu surface, oxidation does not automatically happen, the activation energies of 3.2 eV (FS) or 2.0 eV (SE) would have to be exceeded. Another way to prevent Cu oxidation is to transfer and accumulate excess electrons at the Cu surface as such those negatively charged ions will make the adsorbed oxygen much more unstable, as even after combining with the oxygen atom, the majority remained at the surface. Then coulomb repulsion occurs between the negatively charged copper and the oxygen anions therefore preventing the adsorbed oxygen from entering into the bulk lattice of copper [49]. Copprint is already making an oxidation-free copper nanoparticle ink with an exclusive chemical sintering agent which causes a chemical reaction in nano copper particles, preventing oxidation [27]. Test of oxidation has been done for copper by sintering two printed lines in anaerobic and aerobic conditions and the results show an enhanced oxide formation for the one done in aerobic conditions, especially for elevated temperature [45][50]. Nevertheless, it experienced a degradation of the efficiency, fill factor, and open circuit voltage and a decrease of series resistance with increasing sintering temperature from 175℃ [50].

Table 2:Cost and properties comparison of copper (Cu), silver (Ag), and nickel (Ni) [24]

Parameters	**Ag**	**Cu**	**Ni**
Conductivity (10^6 $S.m^{-1}$)	61.4	59.1	13.9
Density ($mg.cm^{-3}$)	10.5	8.9	8.9
Typical cost ($\$.kg^{-1}$)	431.0	4.5	14.2

In the above table, we compare the cost and properties of copper (Cu), silver (Ag), and nickel (Ni). Copper has a higher resistivity of 3.7% than Ag, but it costs around 100 times less, which is an important factor in cost reduction [24].

As stated previously, copper is a deep-level contaminant that diffuses quickly into silicon and easily reacts with it, causing device deterioration and failure. As for SHJ solar cells, TCO is put between the silicon and the metal contacts, and TCO has been tested as a Cu diffusion barrier. Indium tin oxide (ITO) film and indium tungsten oxide (IWO) film are the two components studied for TCO and both of them resulted to exhibit excellent copper diffusion barrier characteristics, eliminating the need for a separate barrier layer [46].

Chapter2: Methods and Techniques

The methods and techniques used in this thesis are described in this chapter. First the dispenser printing for the metallization of SHJ solar cells, then some measurement methods, and afterward the characterization of solar cells.

1) Dispenser printing metallization

Dispensing is still an emerging technology. To dispense a paste a strong understanding of how the parameters (pressure, height of the nozzle, speed, paste viscosity) are related is ineluctably needed. The machine consists of a robot connected to a laptop with a software named Musashi or teaching pendant (programming device) and a pressure source. This software permits to adjustment of nozzle position and height, where it should go, and the running speed. The initial stage of this process involves configuring a program within the software that instructs the robot on how to carry out the printing procedure on the substrate; subsequently, this program can be transmitted to the robot for execution. The pressure is calibrated by using a pressure source machine, and during program execution, the robot, which is already linked to the pressure source, communicates the timing to release the predetermined pressure to the syringe and nozzle containing the pastes (see **Figure 3-1**). After that, the width of the lines, and their continuity status are evaluated by using a microscope.

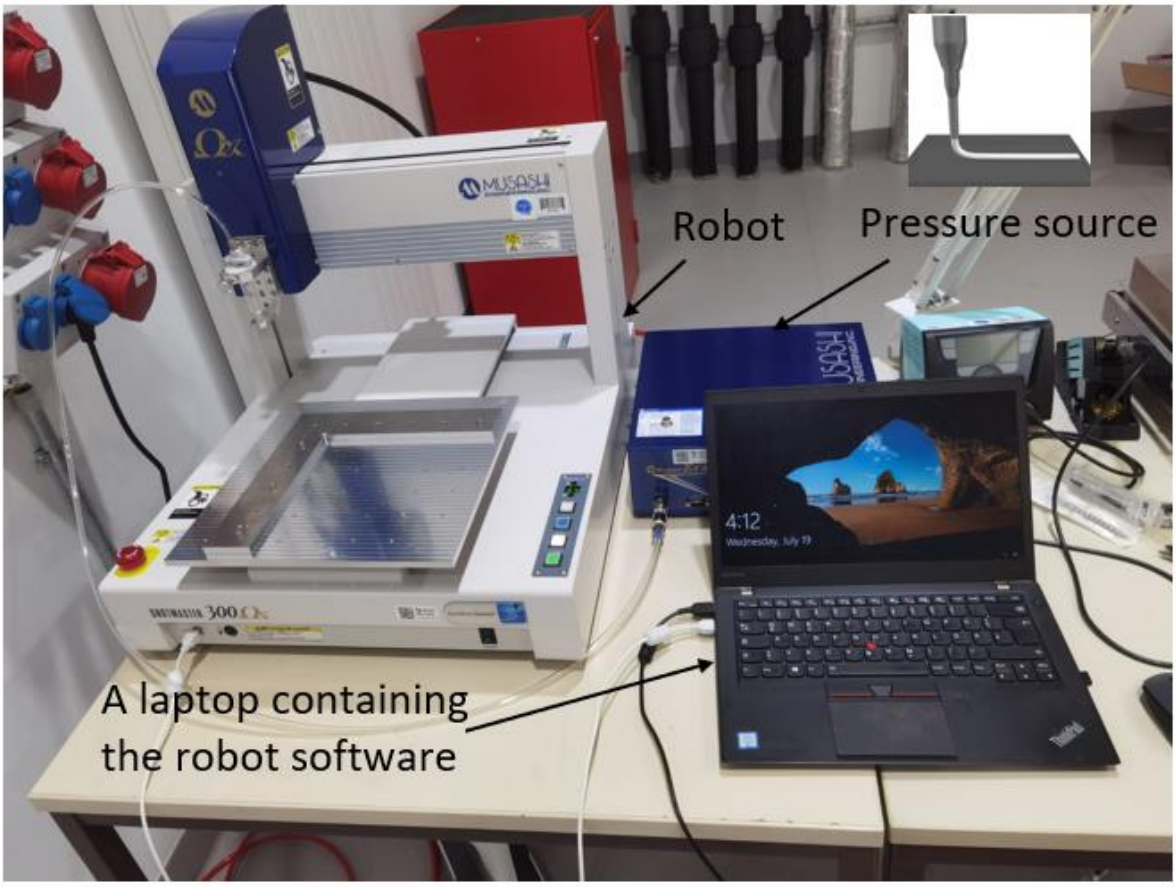

Figure 2-1: Set up dispenser printing

2) Finger conductivity measurement

As resistivity is the reciprocal of conductivity, the resistivity of the dispensed copper fingers is measured by using the 4-point probe method. Unlike the 2-point probe method, which is different, the 4-point probe method is commonly employed for measuring finger resistivity. This technique aids in eliminating the influence of measurement setup resistance and cable interference from the obtained results, a benefit not achievable with 2-point measurements. The 4-point probe method uses a chuck with four equally spaced contacting bars placed on the wafer with fingers (see **Figures 3-2** and **Figure 3-3**). The working principle is that current is applied on two outer probes and the voltage drop is measured between the two inner ones when the current flows in the lines. By measuring this voltage drop and the current, the resistivity can be calculated and recorded.

To realize this experiment, the following setup was made:

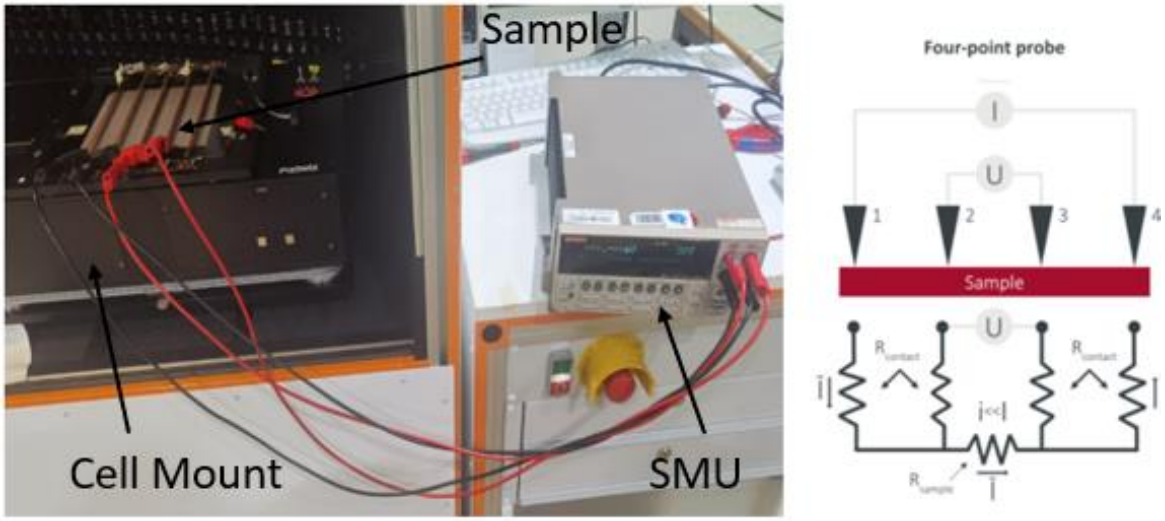

Figure 2-2: Set up of four-point probes measurement

This setup is composed of a source measure unit (SMU) run by a Python program and the sample (solar cell with finger) is placed on the cell mount of LOANA. Then the contact frame is placed on the sample and put on the cell mount. This chuck is connected to the SMU. When the Python program is started, the set current (0.3 mA to 0.8 mA) is sent from the SMU to the outer probes, and the voltage drop between the two inner probes is measured. For accurate finger resistance measurement, six voltage measurements are taken and the corresponding resistances are recorded. Subsequently, the average resistance is calculated based on the number of fingers measured. To get the resistance Rf (in Ω) of one finger, the average resistance is multiplied by the number of fingers since they are in parallel connected in the measurement circuit. Then it is divided by the length of the finger Lf (in cm) to get the resistivity ρ f (in $\Omega.cm^{-1}$) as shown in the formula (1):

$$\rho f = \frac{Rf}{Lf} \quad (1)$$

3) Solar cell characterization

The characterization of the solar cells is done with the LOANA system from pv-tools at IEK-5 (see **Figure 3-4**). This LOANA measurement system from pv-tools integrates several measurements such as J(V)-characteristics, external quantum efficiency (EQE), reflection R,

electroluminescence, internal quantum efficiency IQE...etc. For this research, the system is used to measure mainly the J(V)-characteristics and electroluminescence (EL). The parameters such as efficiency (η), fill factor (FF), pseudo fill factor (pFF), open-circuit voltage (V_{oc}), short-circuit current density (J_{sc}), EL, and series resistance (R_s) are discussed in this thesis. A JV-curve is also included. recorded in two sweeps, one from an open circuit, and one from a short circuit. A typical J-V curve at 1 sun with **Figure 3-3** depicts the maximum power point (MPP).

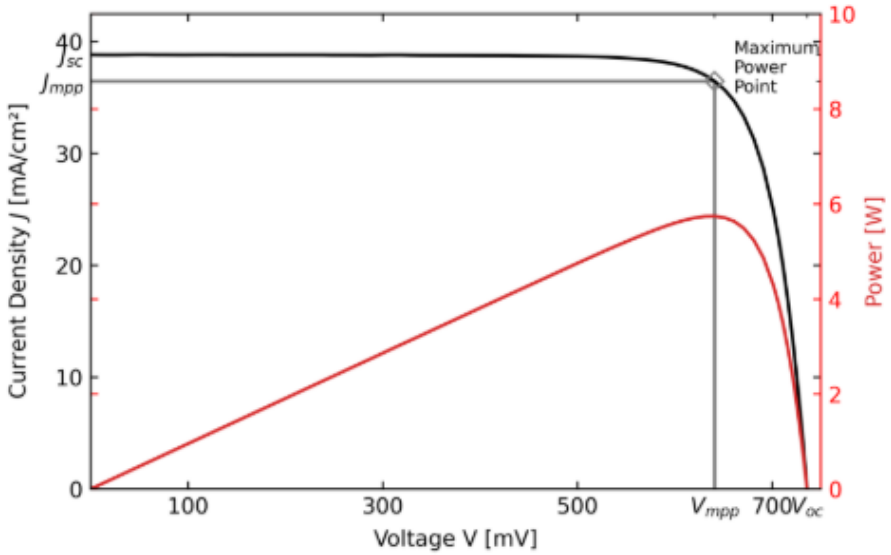

Figure 2-3: Exemplary light J-V curve[32]

The power conversion efficiency (η) is the most important parameter. It is defined as the ratio of obtained power at the maximum power point (MPP) over input power Pin

$$\eta = \frac{\mathrm{P}mpp}{\mathrm{P}in} = \frac{\mathrm{V}mpp * \mathrm{J}mpp}{\mathrm{P}in} \quad (2)$$

The input power (P_{in}) is defined by a reference spectrum corresponding to the AM 1.5G and is delivered by a Wave-labs Sinus 210 LED light source and equals Pin = 1000W.m^{-2} [33]. J_{mpp} is the current density at the maximum power point, and V_{mpp} is the voltage at the maximum power point.

Fill Factor *(FF)* is another important parameter, which measures through its squareness shape (fig above), that describes the relationship of MPP power and the product from V_{oc} and J_{sc}, the quality of a solar cell. The closer to 1 is the FF the better is the cell [51]

$$FF = \frac{\mathrm{V}mpp * \mathrm{J}mpp}{\mathrm{J}sc * \mathrm{V}oc} \quad (3)$$

Then equation above can be expressed as:

$$\eta = \frac{\mathrm{J}sc * \mathrm{V}oc * FF}{\mathrm{P}in} \quad (4)$$

The *pFF* is calculated in the same manner as the *FF* by first shifting the $J_{sc}V_{oc}$ curve to the Jsc[32]. To determine the series resistance with the LOANA measurement system the multi-light method has been established, which is described in more detail by Fong *et al* [52].

For electroluminescence (EL) images, a camera captured them when a voltage was applied to the solar cells. Because it is easier to maintain a constant current than a constant voltage, 0.5 A and 8 A forward currents were used. Applied to the solar cells, the light emitted was captured using a CCD camera. The camera detects light between 900 and 1200 nm. The electroluminescence photos depict cracks in the wafer as well as resistance effects (see **Figure 4-7**).

Figure 2-4:LOANA measurement system from pv-tools for characterization of SHJ solar cells performance [53]

4) Light soaking

Since a degradation of the characterized solar cells happened, light soaking was done to repair them. When light soaking is performed on them, their performance is measured again. The light-soaking effect is the result of constant illumination, which increases the power conversion efficiency of the investigated SHJ solar cells [54].

Figure 2-5: Light soaking machine at IEK-5

For this experiment, fast light soaking was made on the characterized solar cells (~ 90 s). During the process, an LED-based light source with an input intensity of 55 $kW.m^{-1}$ at about 175˚Cis the condition at which the light soaking of the solar cells was done.

Chapter3: Experimental work and results

Since silver paste used as metallization paste for silicon solar cells, is scarce and its price fluctuates greatly. This will make solar cell production more expensive, therefore there is an urgent need to solve this problem. Copper is considered a great alternative to silver to reduce/avoid silver consumption in solar cell production. In this study, the use of copper paste and its process conditions on SHJ solar cells are investigated. dispenser technology is used for printing the copper paste and dispenser parameters are also studied for fine-line printing.

In this chapter, first, the paste properties and dispensing parameters are related, then the evaluation of the performance of the copper fingers depending on the sintering conditions is presented. Secondly, the application of the sintering conditions of the copper fingers to some solar cells is investigated. Then, the possibility to improve their performance by light soaking. Lastly, the performances of solar cells metalized with dispensed copper (made experimentally) are also studied and compared with other SHJ solar cells with Ag screen-printed metallization.

1) Paste properties

This research focuses on dispensing copper paste (LF-380) from Copprint on the silicon surface (c-Si wafer), on TCO (SHJ solar cells without metallization), and SHJ solar cells. The copper paste that is used in this experiment has as properties of uncured materials: a density of 3.75 $g.ml^{-1}$ and a viscosity of 14,3 rpm, $Pa.s^{-1}$ (kcps) at 25°C[55]. It is stored in a fridge at about -20°C. To use it, it has to be warmed up, then it is mixed in the mixer for 165 s, 800 rpm. Once the fingers are made, they are dried on a hot plate, and additionally, for copper fingers, the sintering process is followed up, in an anaerobic condition, to remove its contained solvent. Subsequently, their properties like finger resistance, finger width, and finger homogeneity are measured.

Sintering is the process of curing under a specific temperature to evaporate the solvent contained in the paste and make electrical contact between particles. It is worth noting that for the sintering, the evaporation temperature of the solvent in the paste determines at which temperature fingers become conductive, hence solvent with the lowest evaporation temperature is the best. The most important is to get as low as possible resistance of the printed fingers at the lowest possible temperature [56]. The paste producer provides information for the sintering conditions [27] and for the copper that is used (LF-380), the information from the producer for the sintering is 300°C for 5 s [55] The sintering of copper is done in an anaerobic condition, to avoid any contact with the air oxygen when removing the solvent.

2) Dispensing parameters

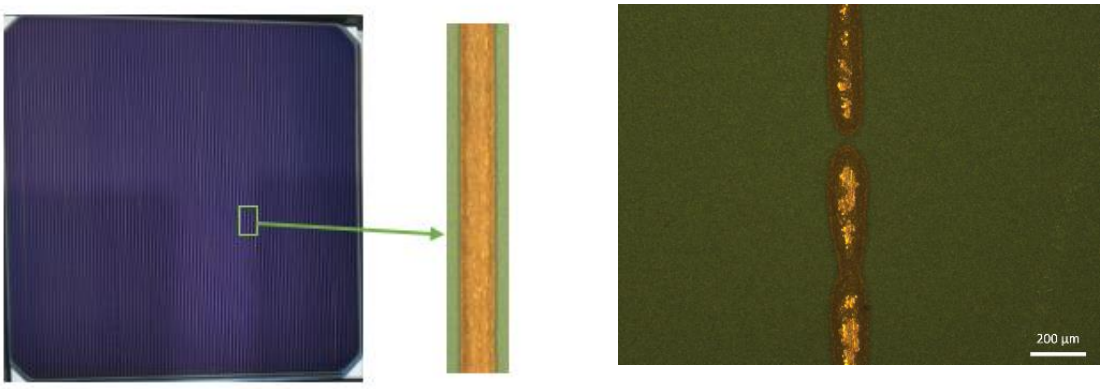

a) SHJ solar cell metallized with dispensed copper paste

b) Disruption of dispensed copper fingers

Figure 3-1: Dispensed copper fingers on SHJ solar cells

Figure 4-1 shows in a) a continuous copper finger (150 µm) is dispensed. In b) a dispensed copper finger with interruptions is shown. The copper was dispensed on metallization free solar cells to establish the metal contacts (fingers).

The finger characteristics depend on a set of dispensing parameters and these parameters (pressure, speed, height of height), and these parameters cannot be adjusted individually.

Depending on the characteristics of the fingers that have to be made, the relationships between the various parameters that are very important for producing a particular finger geometry, especially a fine line, are closely related:

- firstly, the effect of changing the speed at constant nozzle height and pressure, which shows that at low speed the applied paste rolls up and becomes wider, then with increasing speed it is observed that the line becomes finer and finer until a certain limit where it starts to break.
- secondly, the same observation was made with changing nozzle height and constant pressure and speed. This means that a low nozzle height leads to broader lines, whereas when the height is increased, the fingers become finer and finer. At a certain height, it then starts to break the line.
- thirdly, with alternating pressure and constant nozzle height and speed, it was found that with low pressure there are interruptions, while with increasing pressure there is a continuous and fine line up to a certain level, at which there are interruptions again. In addition, to understanding these basics, at the next level, one can begin to study the effects

of changing two parameters and keeping one parameter constant on the line geometry. Then one can also practice the effects of changing three parameters on a fine line, at the highest level

However, challenges are inevitable during the dispensing process. Especially if it is to draw very thin lines. The problems can come from both the paste and the dispensing machine. Below are some of the challenges:

- Based on our observations, we have noticed that the copper paste tends to gradually dry out over prolonged usage (which depends a lot on operation conditions). Then more pressure is needed to extrude the paste and even some parameters change.
- The paste may also contain some bubbles, and these bubbles cause interruptions along the lines when dispensing (see **Figure 4-1 b)**). Bubbles present in a paste can lead to disruptions in finger formation during the dispensing process due to their interference with the uniform flow and deposition of the paste material
- The paste may contain some particles that are larger than the nozzle and clog it.
- The surface of the substrate may not be uniform, changing the width of the produced fingers from a higher level to a lower level, which in turn leads to many difficulties in obtaining continuous and homogeneous fingers for the deeper substrate.
- A nozzle height should be redefined from the thickness of the substrate ...etc.

3) Study of the sintering conditions on copper fingers' resistivity

Appropriate sintering condition is the key for better performance of copper fingers/busbars and here the resistance of copper fingers is evaluated after sintering them in different conditions. The fingers studied are dispensed on the wafer and their resistivity was measured through the four-probes method. Understanding how resistant they are, helps to know if they are good enough to work on a solar cell.

Firstly, the copper fingers were treated in different sintering temperature conditions. This aims to figure out the dependence of the sintering temperature on the conductivity of the dispensed copper fingers. After dispensing the fingers follow up the drying process (100°C for 2 minutes) and then the sintering. The sintering time is 5 s and the following are the different sintering temperatures: 280, 300, 320, 360, and 380°C.

Secondly, we proceed, similarly to the previous experiment, to sinter the dispensed copper fingers in different sintering time conditions. The sintering temperature is 300°C and

the following are the different sintering times: 5, 12, 15, 20, 30, and 40s. This consists of figuring out the influence of different sintering times on the conductivity of the dispensed copper fingers.

.

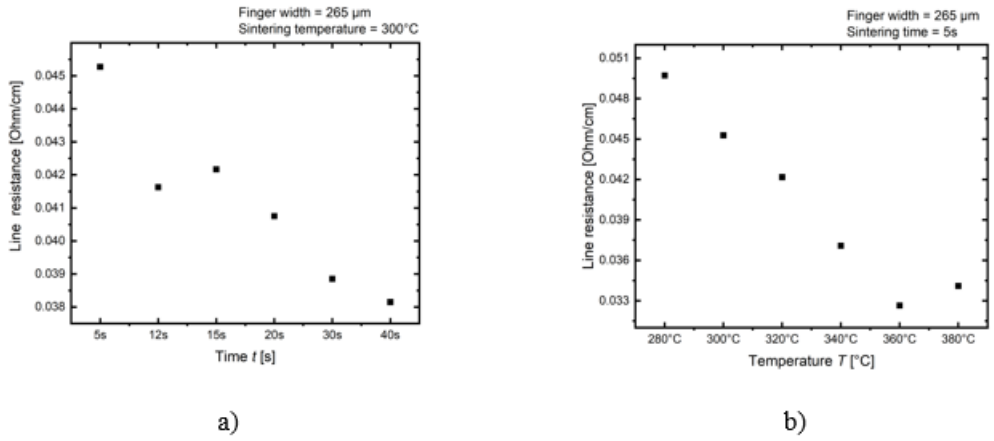

Figure 3-2: Line resistance to sintering time a) and sintering temperature b).

Figure 4-2 shows a plot of the line resistance of copper fingers to sintering time a) and to sintering temperature b). Both of the figures show generally a decrease in line resistance with, respectively, increasing temperature and increasing sintering time. precisely, it can be observed that:

- In the graph a) depicting line resistance against sintering time, there is a notable reduction in line resistance from 5 to 12 s of sintering time, followed by a slight increase between 12 and 15 s. From 15 to 40 s of sintering time, the line resistance consistently decreases in a linear pattern.
- In the graph b) correlating line resistance with sintering temperature, a linear decline in line resistance is evident between sintering temperatures of 280 and 360°C. However, a subsequent rise in line resistance occurs at a sintering temperature of 360°C.

Dispensed pastes (Cu paste and Ag paste) are analyzed here to determine some of their properties. The line resistance of the dispensed Ag paste and Cu paste is measured and compared with other printing technologies. In addition, the behavior of the distributed pastes on the wafers and the TCO is also evaluated (see **Figure 4-3**).

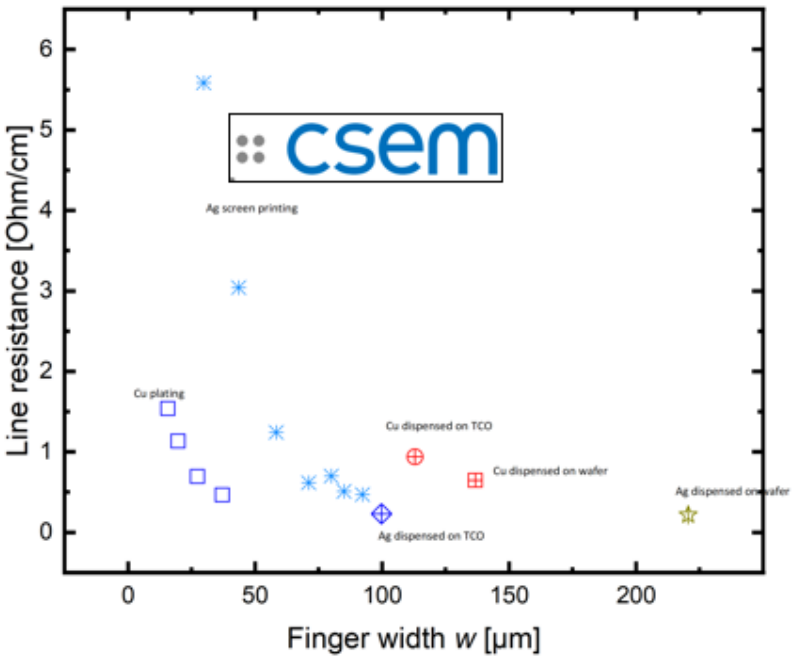

Figure 3-3: Line resistance to finger width

Figure 3-3 gives a comparison of the line resistances at the finger width of dispensed Ag paste and Cu paste compared with other printing technologies. Data for other printing technologies (screen printing, Cu plating) were obtained from the Swiss Centre for Electronics and Microtechnology (CSEM). Differences in wafer shape and TCO are also shown for distributed pastes. Firstly, we can see that the dispensed paste analyzed is large (over 100µm). Secondly, by comparing the pastes dispensed on the wafer and the TCO, we can see that, the paste dispensed on the wafer spreads much more widely than that on the TCO (NB: all these dispensing's were carried out using the same parameters). Line resistance is shown to decrease progressively with increasing finger width for screen printing and Cu plating. However, if we compare their line resistance, copper plating offers a lower line resistance than the other technologies. We have included the results from this study's copper dispensed fingers creation in the published graph about width versus line resistance by CSEM. As far as dispensed pastes are concerned, we can see that they have a slightly higher resistance than the others printing technology, particularly dispensed paste on wafers.

4) Sintering of SHJ solar cells

In this part, we subjected finished standard silicon heterojunction (SHJ) solar cells (sourced from Tongwei) to the same treatment conditions previously applied to our copper fingers. This step aimed to assess whether the solar cells do not degrade at the copper finger treatment conditions and understand the resulting impact on their performance. Subsequently, light soaking was administered to all cells after various treatments to recover their performance post-treatment and observe the effect of this light soaking on SHJ solar cells following the performance decline caused by sintering.

A total of 24 solar cells were subjected to different sintering conditions to explore how copper finger sintering conditions influence their performance. **Figure 4-4** shows several SHJ solar cells underwent treatments as follows: 4 pieces of solar cells at 280°C, 4 pieces of solar cells at 320°C, and 4 other pieces of solar cells at 360°C, and the sintering time for all of the cells was 5s. **Figure 4-5** shows other solar cells treated as follows: 4 pieces of solar cells at 5 s, 4 pieces of solar cells at 20 s, and 4 pieces of solar cells at 40 s, and the sintering temperature for all the cells was 300°C. Performance measurement was carried out before and following sintering, utilizing the LOANA system (refer to **Figure 3-3**). Additionally, a standard light curing procedure was applied to all cells, followed by performance measurements (refer to **Figure 3-5**).

Figure 4-4 and **Figure 4-5** show graphs of the results of the different treatments of the solar cells. Six parameters (efficiency, V_{oc}, J_{sc}, *pFF*, *FF*, R_s) are mainly considered. As stated previously, the result is divided into three main sintering temperature and time conditions. On the following two figures, for each sintering condition, there is a subgroup for before sintering (BS), after sintering (AS), and after light soaking (LiSo). The box chat in grey color, red color, and blue color represents the results before treatment, after treatment, and after light soaking.

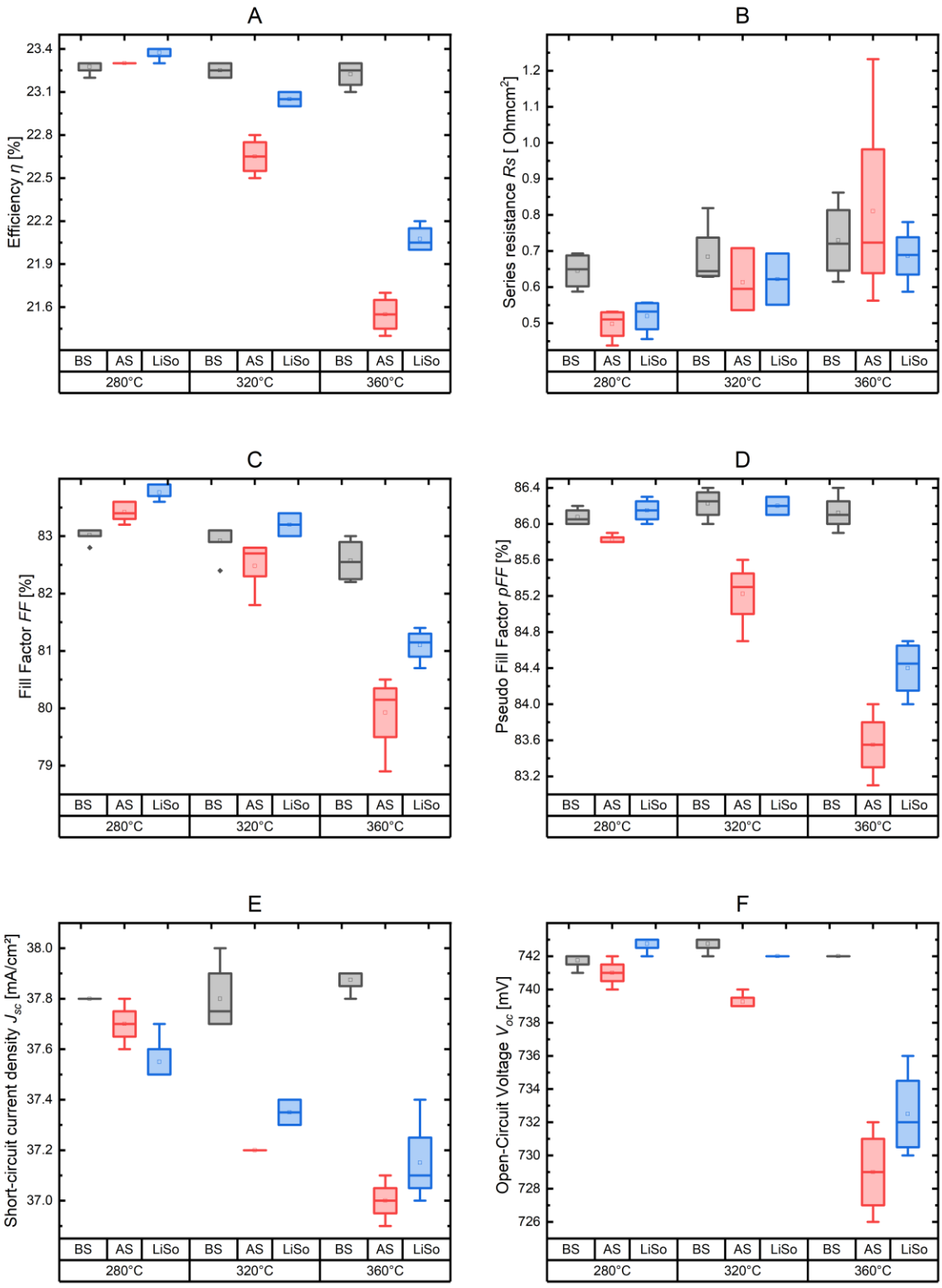

***Figure 3-4*:** Standard solar cells sintered in different temperature conditions and light-cured

Figure 3-4 presents a plot illustrating the relationship between distinct parameters and sintering temperature conditions. The graph offers compelling evidence of a consistent decline (whether slight or significant) in solar cell performance across various parameters as the temperature increases, though some exceptions apply. Similarly, upon subjecting the data to light curing, a pervasive improvement (slight and/or significant) can be observed in the parameters of these solar cells.

In particular, the following observations can be made from the graphs:

- Graph A (Efficiency vs. Sintering Temperature): The efficiency of the batch treated at 280°C shows a slight increase after sintering and a further increase after light soaking. For the 320°C treatment, efficiency decreases significantly, then rises again after light soaking. And at 360°C sintering temperature, the efficiency undergoes a substantial decline, followed by an improvement after light soaking. The efficiency of all cells at the initial stage ranges narrowly between 23.1 to 23.3%. However, they were treated differently and the average loss is more noticeable at 320°C and 360°C treatment temperature, up 0.9% average efficiency loss.
- Graph B (Series Resistance vs. Sintering Temperature): As the trend observed in previous results indicating decreasing of dispensed Cu line resistivity with higher sintering temperature, the series resistance (R_s) shows a decrease after treatment at all three sintering temperatures. Notably, this decrease is less pronounced with higher temperatures. Light soaking has a modest positive impact on the treated cells' performance.
- Graph C (Fill Factor vs. Sintering Temperature): At 280°C sintering temperature, the fill factor (*FF*) increases, with a more significant increase after light soaking. For 320°C and 360°C treatments, *FF* decreases, particularly markedly for 360°C. Light soaking leads to a rise in the post-treated solar cells' *FF*.
- Graph D (Pseudo Fill Factor vs. Sintering Temperature): Following treatment at all three sintering temperatures, there's a decrease in the pseudo-fill factor (*pFF*), with the decrease being more pronounced at higher temperatures. A rise in *pFF* is observed after light soaking for the post-treated solar cells.
- Graph E (Short-Circuit Current Density vs. Sintering Temperature): A consistent decrease in short-circuit current density (J_{sc}) is observed after treatment at all three sintering temperatures, with a more substantial decrease at higher temperatures. Light soaking doesn't improve the J_{sc} for cells treated at 280°C; however, it enhances Jsc for cells treated at 320°C and 360°C.

- Graph F (Open-Circuit Voltage vs. Sintering Temperature): Similarly, after treatment at all three sintering temperatures, there's a decrease in open-circuit voltage (V_{oc}) for the post-treated solar cells, with the decrease being most significant at 360°C. Light soaking applied to the 280°C-treated cells restores their V_{oc} above the pre-treatment level. For cells treated at 320°C and 360°C, light soaking enhances V_{oc}, particularly for the 320°C treatment temperature.

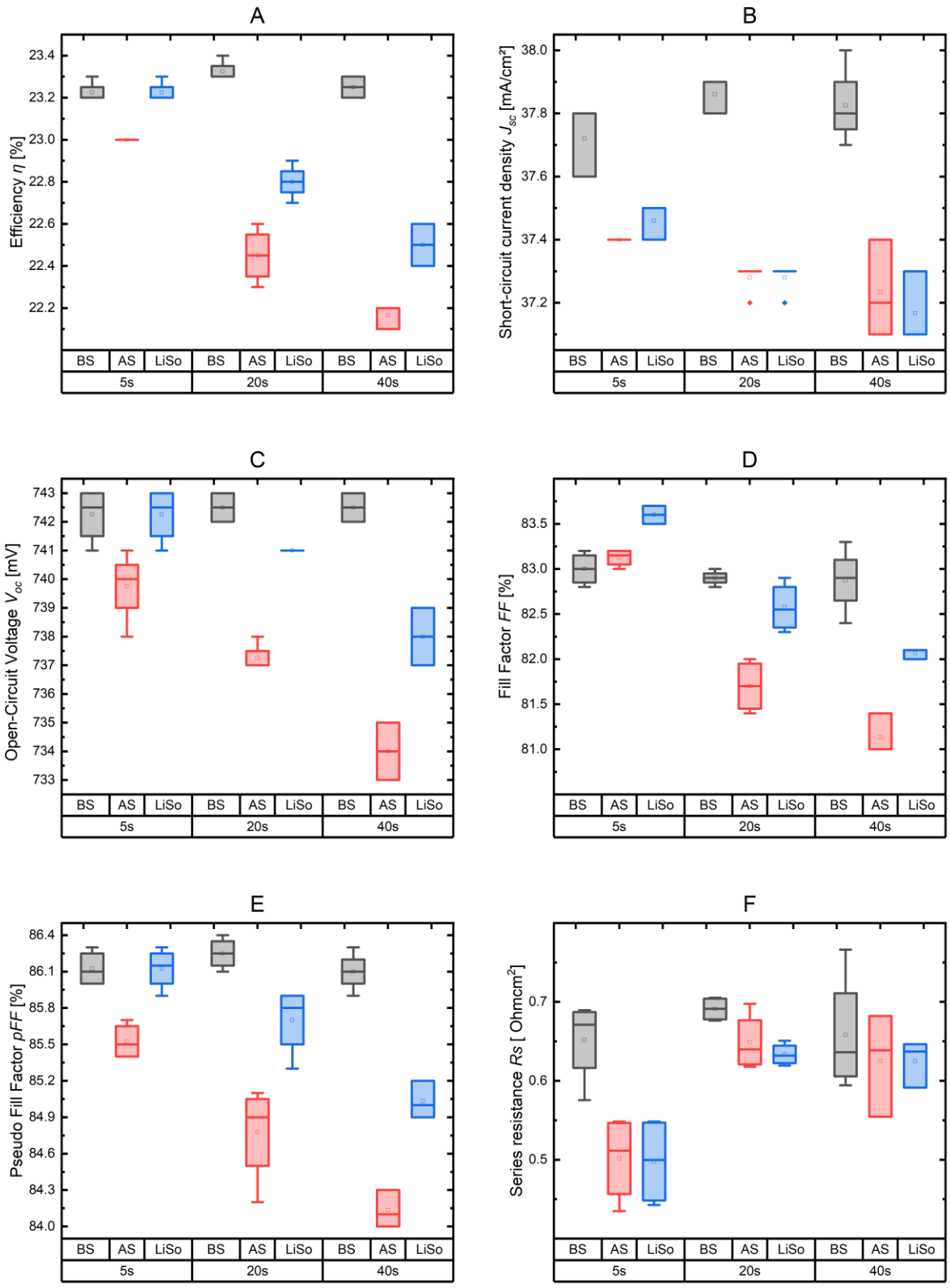

***Figure 3-5*:** Standard solar cells sintered in different time conditions and light-cured

Figure 3-5 shows a relationship between a specific solar cell parameter and the sintering time conditions. The parameter variations that have been observed closely reflect those that have been examined previously about the sintering temperature settings. It is noticeable that the parameters show smaller variations in this particular figure.

The presented graphs offer the following insights:

- Graph A (Efficiency vs. Sintering Time): The efficiency of the batch treated for 5s decreases post-sintering but recovers to its initial level after light soaking. For 20s and 40s treatments, there's a notable drop in efficiency, especially pronounced for the 40s treatment, followed by enhancement after light soaking. The efficiency of all cells initially ranges narrowly between 23.1% to 23.3%. However, since they were treated differently the average loss is more noticed at 20s and 40s treatment time, up 0.8% average efficiency loss.
- Graph B (Short-Circuit Current Density vs. Sintering Time): A consistent decline in short-circuit current density (J_{sc}) is observed across all three sintering times, with the most significant decrease at the 40s. Light soaking has minimal impact on Jsc for cells treated for 5s and 20s, but slightly enhances J_{sc} for some cells treated for 40s.
- Graph C (Open-Circuit Voltage vs. Sintering Time): Similarly, all three sintering times lead to reduced open-circuit voltage (V_{oc}) in post-treated solar cells, with the most noticeable decrease at the 40s. Light soaking restores V_{oc} for cells treated for 5s while enhancing V_{oc} for cells treated for 20s and 40s.
- Graph D (Fill Factor vs. Sintering Time): At 5s sintering time, fill factor (*FF*) experiences a slight increase, followed by a more significant rise after light soaking. Conversely, for the 20s and 40s treatments, *FF* decreases significantly, especially in the 40s. Light soaking positively affects the FF of post-treated solar cells.
- Graph E (Pseudo Fill Factor vs. Sintering Time): Post-treatment at all three sintering times leads to decreased pseudo-fill factor (*pFF*), with the reduction being most pronounced at longer sintering times, particularly at the 40s. Light soaking subsequently raises *pFF* for the treated solar cells.
- Graph F (Series Resistance vs. Sintering Time): In contrast to the prior results indicating decreased line resistivity with higher sintering time, series resistance (R_s) decreases for all three sintering times. However, this decrease is less significant as the sintering time increases. Light soaking doesn't significantly impact the performance of the treated cells in terms of series resistance.

5) SHJ solar cells metalized with dispensed copper metallization

As the aim is to evaluate the performance of dispensed copper metallization as an alternative to silver on SHJ solar cells, SHJ solar cells metalized with dispensed copper were made. After studying dispensed copper fingers (**Figure 4-3**) and solar cells treated in different sintering conditions (**Figure 4-4** and **Figure 4-5**), here SHJ solar cells are studied (from Tongwei), on which: first; 3 solar cells with Ag paste is screen-printed on the front side and then dispensed copper paste at the rear side, second, 2 solar cells Ag paste is screen-printed on the rear side and then dispensed Cu on the front side with 1.5 mm finger pitch and 4 solar cells Ag paste is screen-printed on the rear side and then dispensed Cu on the front side with 2.5 mm finger pitch, and third, both sides dispensed Cu where we have 2 cells with 1.5 mm finger pitch and 1 cell with 2 mm pitch. Approximately 103 fingers are made on all the dispensed Cu metalized solar cells with a pitch of 1.5mm and 2mm. These solar cells are studied in comparison to reference solar cells, including 5 finished solar cells and 3 solar cells on both sides Ag screen-printed. The wafers are M2 size (244.3 cm^2). All the procedures were done, and then their performance was studied with LOANA. Since SHJ solar cells consume more silver, particularly the rear side, replacing it with copper could be very significant in reducing the SHJ solar cells' silver consumption.

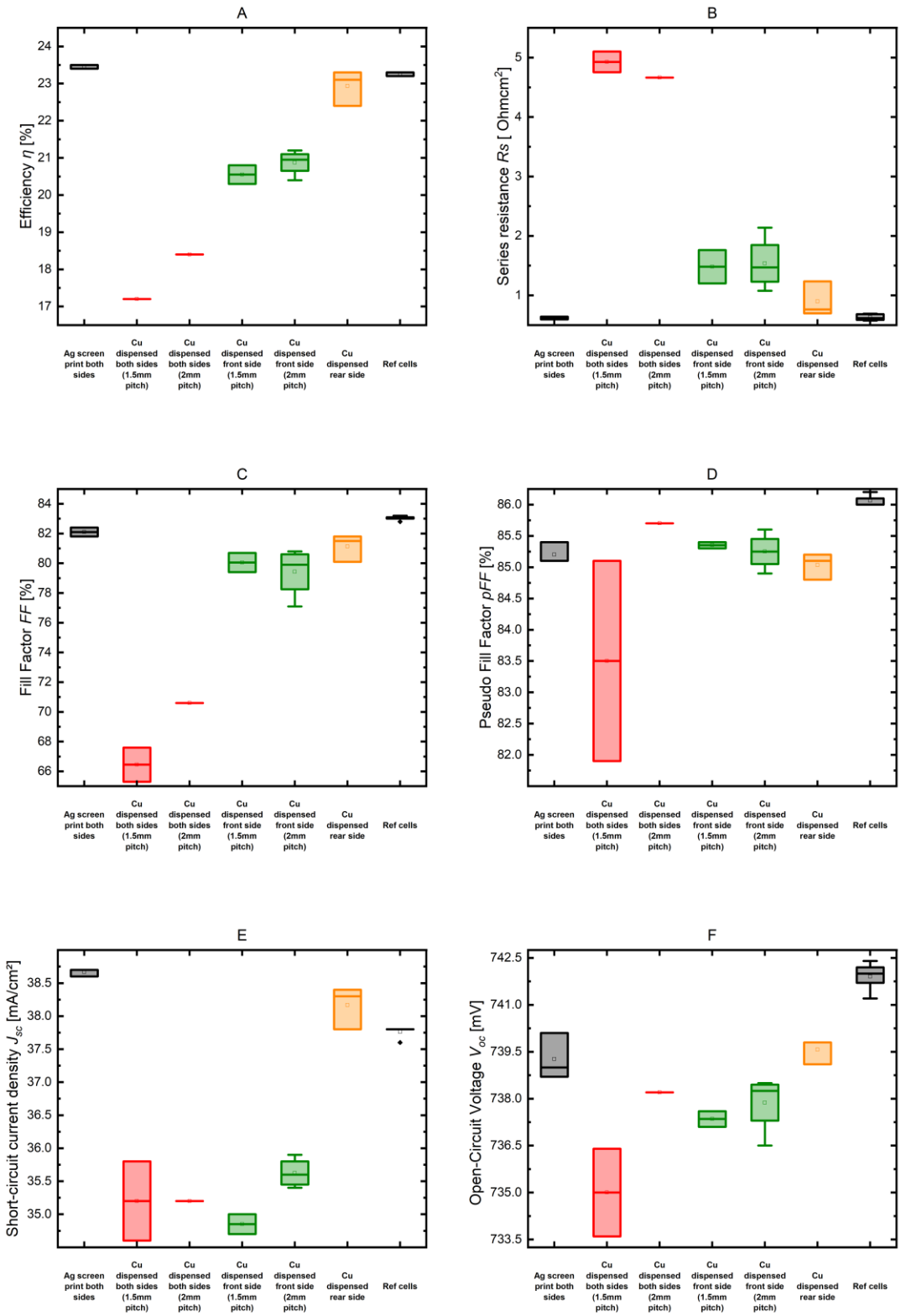

***Figure 3-6*: Results of Cu dispensed cells and Ag screen printed characteristics**

Figure 4-6 showcases the performance parameters (Efficiency, Jsc, Voc, Rs, FF, pFF) of various solar cell types: reference solar cells, Ag screen-printed on both sides' solar cells, Cu-dispensed front side solar cells (with 1.5 mm pitch and 2 mm pitch), Cu-dispensed rear side solar cells (with 1.5 mm pitch), and both sides dispensed Cu solar cells (with 1.5 mm pitch and 2 mm pitch). The observations are as follows:

- Graph A (Efficiency Plot): Compared to reference cells, most Cu-dispensed SHJ solar cells exhibit lower efficiency, while Ag-screen printed SHJ cells on both sides show similar efficiency. Among Cu-dispensed SHJ cells, those with Cu dispersion on the rear side display the highest efficiency, followed by front-side dispersion and both-side dispersion, with 1.5 mm pitch cells showing the lowest efficiency.
- Graph B (Series Resistance Plot): Cu-dispensed SHJ cells generally have higher series resistance than reference cells, while Ag-screen printed cells have comparable resistance. Double-sided Cu-dispensed cells, especially with 1.5 mm pitch fingers, show notably the highest series resistance. Back-side Cu-dispensed cells exhibit the lowest series resistance, followed by front-side cells, and both-side cells have the highest resistance.
- Graph C (Fill Factor Plot): Fill factor (*FF*) is lower for both-side Cu-dispensed and Ag screen-printed SHJ cells compared to reference cells. Both-side Cu-dispensed cells, particularly with 1.5 mm pitch fingers, exhibit the lowest *FF.*
- Graph D (Pseudo Fill Factor Plot): Cu-dispensed and Ag screen-printed SHJ cells generally display lower pseudo fill factor (*pFF*) than reference cells. Among Cu-dispensed cells, those on both sides with 1.5 mm pitch fingers exhibit the lowest *pFF*. Back-side Cu-dispensed cells with 2 mm fingers have the highest *pFF,* followed by front-side cells, and both-side cells with 1.5 mm pitch have the lowest *pFF*.
- Graph E (Short Circuit Current Density Plot): Ag-screen printed SHJ cells on both sides have the highest short circuit current density (J_{sc}), followed by back-side Cu-dispensed cells

(with higher J_{sc} than reference cells). Front-side and both-side Cu-dispensed SHJ cells have the lowest Jsc, particularly those with 1.5 mm pitch fingers.

- ❖ Graph F (Open Circuit Voltage Plot): All cell types, except reference cells, display lower open circuit voltage (V_{oc}). Among them, both-side Cu-dispensed SHJ cells with 1.5 mm pitch exhibit the lowest V_{oc}.

When it was observed for Cu dispensed solar cells front side and both sides with 2mm pitch and 1mm pitch, those with 1.5 mm pitch gives better performance.

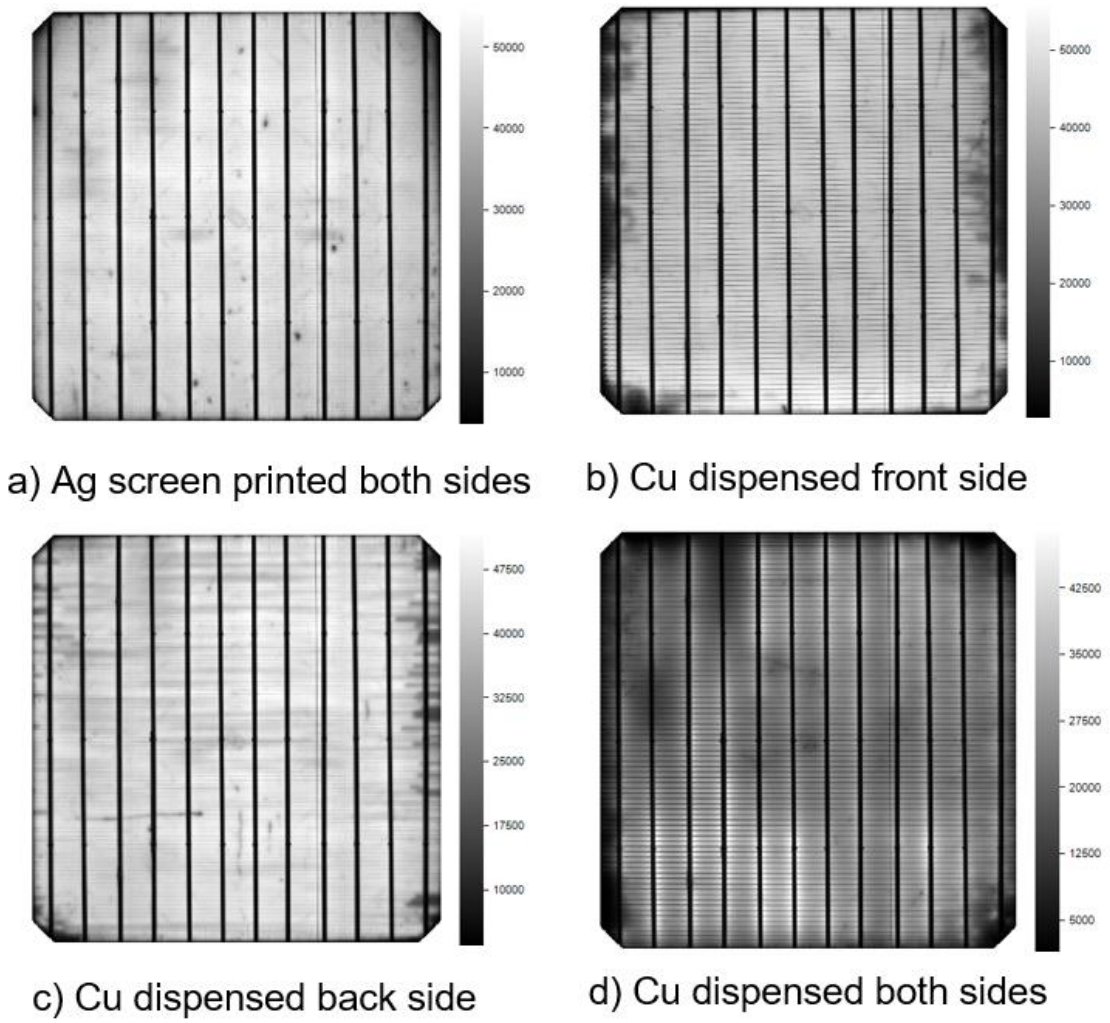

Figure 3-7: In a) is an exemplary EL image for reference solar cells, in b) is an exemplary EL image for front side dispensed Cu solar cells, in c) is an exemplary EL image for rear side dispensed Cu solar cells, and in d) is an exemplary EL image for both sides dispensed Cu solar cells

Figure 4-7 provides information about electroluminescence (EL) images of the SHJ solar cells made, metalized with dispensed copper, in comparison to the reference solar cells

EL images. It can be noticed that all the EL images with dispensed Cu solar cells have some dark area, particularly at the edges. Which is worst for both sides dispensed Cu. This explains the bad conductivity of the fingers and the low quality of the printing.

Chapter4: Discussion and interpretation

In this chapter, the results of the research on dispensed copper metallization for silicon heterojunction (SHJ) solar cells are discussed. The implications of the results were investigated and comparisons with previous studies were made to provide comprehensive knowledge of the performance and potential of dispensed copper metallization in SHJ solar cells.

The results of this research show, on the one hand, the great potential that copper metallization has on SHJ solar cells as an alternative to silver metallization, which makes it an excellent candidate for reducing silver consumption and the cost of solar cell production. On the other hand, the state of development of dispenser printing is estimated to be a great alternative to traditional screen printing due to its enormous advantages mentioned before. Realistically, many efforts are still needed to further improve this technology.

In comparison to what Pospischil *et al.,* 2022 reported, a finger width of 17 μm was achieved with dispenser technology [22], while in this case, the finger width is above 100 μm. This is due to the limitations of our setup. The precision of dispensing as emerging technology, the paste viscosity, dispensing rate, and adaptability to substrate variations are critical factors in achieving consistent metallization quality and reducing issues related to poor adhesion. Conclusively, the investigation demonstrated that dispenser characteristics influence the overall quality and effectiveness of dispensed copper metallization for SHJ solar cells.

The investigation of the resistivity of our copper fingers under different time and temperature treatment conditions revealed insightfully that the resistivity of the copper fingers decreases with increasing time and temperature. As the copper paste fingers are mixed with a solvent in their initial state, this prevents any conductivity of the paste. The data show that the resistance of the copper fingers decreases with higher and longer treatment conditions, and that means that a higher sintering temperature and longer duration offers more chances to remove the contained solvent in the paste so that most or all of the particles in the paste can make physical contact and conduct charge carriers efficiently.

Since SHJ solar cells are manufactured at low temperatures, SHJ solar cells from Tongwei were treated at the same time and temperature sintering conditions to know whether the cells would work with these conditions. Surprisingly, the results (**Figure 4-4** and **Figure 4-5**) show that the cells work at 280℃, 5s treatment. However, above that condition, the solar cells are damaged. The degradation of the efficiency at higher temperatures and longer treatment times is explained by the gradual decrease from 83.2 to 81% of the fill factor with higher and

longer sintering conditions, as well as the gradual decrease of the open circuit voltage (V_{oc}) with higher and longer sintering conditions. The decrease in V_{oc} means the passivation layer of the solar cells is being damaged. An optimum peak temperature of 325°C is identified with the SHJ passivation quality in [31]. Additionally, performance improvement was achieved after light soaking, which means that some of the instabilities of the cells due to the sintering process were mitigated.

Based on the promising results obtained about copper fingers' performances and the proof that SHJ solar cells work at their treatment conditions, we realized very efficient SHJ solar cells metalized with dispensed Cu, specifically at the rear side. For SHJ solar cells metalized with the rear side dispensed Cu, up to 23.3% efficiency was achieved, for SHJ solar cells metalized with both sides dispensed Cu, 18.4% efficiency is the highest and 21.2 % efficiency for SHJ solar cells metalized with the front side dispensed Cu. 23.3% is also the most efficient SHJ solar cell reference. These results testify that copper could replace silver efficiently for the metallization of SHJ solar cells and even could reach a better performance than silver. However, more improvement and more studies are needed to confirm it. Furthermore, the results obtained provide that Cu dispensed can substitute more than half of the current silver used on SHJ solar cells. Comparatively, Katharina Gensowski *et al* reported that with a dispensed metal grid of pastes, an efficiency of SHJ solar cells of 22.5% ± 0.1% is achieved and this contributed to an efficiency advantage of 0.3 %abs. Compared to the screen-printed grids of paste [41], in this study, there was no gain of efficiency advantages with dispensed copper in comparison to the screen-printed silver paste solar cells.

The higher series resistance explains the lower efficiency and the lower fill factor, specifically for dispensed Cu on both sides of metallization, which as shown in the EL images could be due to some printing issues. Metal contact is already known as one of the causes of series resistance and that leads to a deterioration of the fill factor and efficiency of a solar cell. Therefore, we can conclude that the decrease in efficiency, fill factor, and short-circuit current shown in **Figure 4-6** for the dispensed Cu solar cells is caused by the high series resistance of particularly Cu front side and the two sides, respectively. The lower J_{sc} observed for the dispensed Cu solar cells could be because of the wide fingers on those cells. Except for the Cu dispensed on both sides 1.5 mm finger pitch, the *pFF* is seen to not be significantly affected. The wide fingers explained the lower efficiency of dispensed Cu front-side solar cells compared to dispensed Cu rear-side solar cells. To locate the cause of the higher series resistance of Cu dispensed on both sides of solar cells because they are annealed 2 times (after each side

printing), the Cu dispensed on one side was annealed for a second time to see whether that will increase significantly the series resistance. Surprisingly, that is not the cause. It is worth noting that for this research, the results may be partly wrong because the cells made are busbarless and the reference cells are 5 busbars cells while the chuck we use to characterize them is 12 busbars chuck. The shadow effect on the cells may influence the performance of the cells, affecting the short circuit, the fill factor, and the efficiency.

About the EL images, since they show the defects of a solar cell, it can be observed that the dispensed Cu metalized has defects, particularly at the edges. One can say that it may be due to some printing issues or a bad conductivity of fingers probably caused by issues related to the sintering process.

Conclusion & outlook

In conclusion, dispensed copper metallization is a promising way to reduce the silver consumption for SHJ solar cells. It has been shown that higher and longer sintering conditions lead to a higher finger conductivity for SHJ solar cells. However, it is worth noting that SHJ (Silicon Heterojunction) solar cells have a degradation threshold at temperatures exceeding 280°C. Despite this challenge, it has been observed that a degree of recovery from such degradation can be achieved through the application of light soaking techniques. Significant progress has been made in terms of the viability of using dispensed copper on the rear side of SHJ solar cells, providing a convincing proof of concept. Nonetheless, the utilization of copper dispensing on the front and both sides of SHJ solar cells necessitates further refinement. This includes addressing issues related to the width of the conductive fingers, which requires careful reduction to enhance overall performance.

Nevertheless, further research is needed to evaluate the full potential of dispensed copper metallization for SHJ solar cells including efforts to improve the dispensing process, a degradation study, a reliability study, a diffusion study, and an exact economical study to evaluate the cost benefits.

Bibliography

[1] IPCC, ‘Mitigation Pathways Compatible with 1.5°C in the Context of Sustainable Development’, in *Global Warming of 1.5°C*, Cambridge University Press, 2022, pp. 93–174. doi: 10.1017/9781009157940.004.

[2] ‘The Paris Agreement _ UNFCCC’ : https://unfccc.int/process-and-meetings/the-paris-agreement

[3] ‘Fossil fuels and climate change: the facts | ClientEarth’. Accessed: Jun. 26, 2023. [Online]. Available: https://www.clientearth.org/latest/latest-updates/stories/fossil-fuels-and-climate-change-the-facts/

[4] L. Ibrahim Tanimoune, M. Saidou, and M. Mohamed, ‘UNIVERSITÉ ABDOU MOUMOUNI MASTER THESIS For the certificate of MASTER IN CLIMATE CHANGE AND ENERGY Presented by Study of Potential Sites for Solar PV Power Plant Implementation in the City of Niamey Using GIS Approach’.

[5] I. Renewable Energy Agency, *World Energy Transitions Outlook 2022: 1.5°C Pathway*. 2022. [Online]. Available: www.irena.org

[6] ‘Chapter 2: Sources of CO 2’: https://www.researchgate.net/publication/342986896_Chapter_2_Sources_of_CO2

[7] K. A. Oyewole, O. B. Okedere, K. O. Rabiu, K. O. Alawode, and S. Oyelami, ‘Carbon dioxide emission, mitigation and storage technologies pathways’, *Sustainable Environment*, vol. 9, no. 1. Taylor and Francis Ltd., 2023. doi: 10.1080/27658511.2023.2188760.

[8] C. Breyer *et al.*, ‘On the role of solar photovoltaics in global energy transition scenarios’, *Progress in Photovoltaics: Research and Applications*, vol. 25, no. 8, pp. 727–745, Aug. 2017, doi: 10.1002/pip.2885.

[9] P. J. Verlinden, ‘Future challenges for photovoltaic manufacturing at the terawatt level’, *Journal of Renewable and Sustainable Energy*, vol. 12, no. 5, Sep. 2020, doi: 10.1063/5.0020380.

[10] A. Louwen, W. Van Sark, R. Schropp, and A. Faaij, ‘A cost roadmap for silicon heterojunction solar cells’, *Solar Energy Materials and Solar Cells*, vol. 147, pp. 295–314, Apr. 2016, doi: 10.1016/j.solmat.2015.12.026.

[11] T. Dullweber, L. Tous, and EBSCO Publishing (Firm), *Silicon solar cell metallization and module technology*.

[12] ‘Metal/Semiconductor Ohmic Contacts Technology or Gate Length Series Resistance (ohms)’: https://web.stanford.edu/class/ee311/NOTES/Ohmic_Contacts.pdf

[13] Y. Zhang, M. Kim, L. Wang, P. Verlinden, and B. Hallam, ‘Design considerations for multi-terawatt scale manufacturing of existing and future photovoltaic technologies: Challenges and opportunities related to silver, indium and bismuth consumption’, *Energy Environ Sci*, vol. 14, no. 11, pp. 5587–5610, Nov. 2021, doi: 10.1039/d1ee01814k.

[14] J. Yu *et al.*, ‘Copper metallization of electrodes for silicon heterojunction solar cells: Process, reliability and challenges’, *Solar Energy Materials and Solar Cells*, vol. 224. Elsevier B.V., Jun. 01, 2021. doi: 10.1016/j.solmat.2021.110993.

[15] N. Chen *et al.*, ‘Thermal stable high efficiency copper screen printed back con-tact solar cells’.

[16] A. Razzaq, T. G. Allen, W. Liu, Z. Liu, and S. De Wolf, ‘Silicon heterojunction solar cells: Techno-economic assessment and opportunities’, *Joule*, vol. 6, no. 3. Cell Press, pp. 514–542, Mar. 16, 2022. doi: 10.1016/j.joule.2022.02.009.

[17] M. Green, E. Dunlop, J. Hohl-Ebinger, M. Yoshita, N. Kopidakis, and X. Hao, ‘Solar cell efficiency tables (version 57)’, *Progress in Photovoltaics: Research and Applications*, vol. 29, no. 1, pp. 3–15, Jan. 2021, doi: 10.1002/pip.3371.

[18] M. Taguchi *et al.*, ‘HIT cells - high-efficiency crystalline Si cells with novel structure’, *Progress in Photovoltaics: Research and Applications*, vol. 8, no. 5, pp. 503–513, Sep. 2000, doi: 10.1002/1099-159X(200009/10)8:5<503::AID-PIP347>3.0.CO;2-G.

[19] N. Chen *et al.*, ‘Thermal stable high efficiency copper screen printed back con-tact solar cells’.

[20] T. Wenzel *et al.*, ‘Progress with screen printed metallization of silicon solar cells - Towards 20 μm line width and 20 mg silver laydown for PERC front side contacts’, *Solar*

Energy Materials and Solar Cells, vol. 244, Aug. 2022, doi: 10.1016/j.solmat.2022.111804.

[21] M. Pospischil *et al.*, 'Optimizing fine line dispensed contact grids', in *Energy Procedia*, Elsevier Ltd, 2014, pp. 693–701. doi: 10.1016/j.egypro.2014.08.046.

[22] M. Pospischil *et al.*, 'Applications of parallel dispensing in PV metallization', in *AIP Conference Proceedings*, American Institute of Physics Inc., Sep. 2019. doi: 10.1063/1.5125870.

[23] 'Conductive copper Pastes Portfolio overview', 2021.: http://copprint.com/wp-content/uploads/2021/04/Copprints-product-portfolio-April-2021.pdf

[24] N. Balaji, M. C. Raval, and S. Saravanan, 'Review on Metallization in Crystalline Silicon Solar Cells'. [Online]. Available: www.intechopen.com

[25] 'SunPower ® Module 40-year Useful Life'. [Online]. Available: http://www.sunpower.com

[26] 'SunDrive achieves 26.41% efficiency with copper-based solar cell tech – pv magazine International'. Accessed: Jul. 14, 2023. [Online]. Available: https://www.pv-magazine.com/2022/09/05/sundrive-achieves-26-41-efficiency-with-copper-based-solar-cell-tech/

[27] 'Products – Copprint'. Accessed: Jul. 16, 2023. [Online]. Available : https://www.copprint.com/products/#LF-380

[28] 'Silver accounts for 10% of PV module costs – pv magazine International'. Accessed: Jun. 29, 2023. [Online]. Available: https://www.pv-magazine.com/2021/03/04/silver-currently-accounts-for-10-of-pv-module-costs/

[29] 'itrpv_2023 (2)': https://www.vdma.org/international-technology-roadmap-photovoltaic

[30] 'Silver prices expected to rise by 11% this year – pv magazine International'. Accessed: Jun. 29, 2023. [Online]. Available: https://www.pv-magazine.com/2021/02/12/silver-prices-expected-to-rise-by-11-this-year/

[31] J. Schube, ‘Metallization of Silicon Solar Cells with Passivating Contacts Schriftenreihe der Reiner Lemoine-Stiftung Metallization of Silicon Solar Cells with Passivating Contacts’.

[32] K. R. Ortel, ‘Development of Nanocrystalline Silicon Layers in Silicon Heterojunction Solar Cells presented by’, 2023.

[33] T. Rudolph, ‘Application of Intensive Light Soaking on Silicon Heterojunction Solar Cells and Modules presented by’, 2022.

[34] C. Kunpai, M. G. Kang, H. eun Song, and D. Y. Shin, ‘Fine front side metallisation by stretching the dispensed silver paste filament with graphite nanofibres’, *Solar Energy Materials and Solar Cells*, vol. 169, pp. 167–176, Sep. 2017, doi: 10.1016/j.solmat.2017.05.010.

[35] D. Erath *et al.*, ‘Comparison of innovative metallization approaches for silicon heterojunction solar cells’, in *Energy Procedia*, Elsevier Ltd, 2017, pp. 869–874. doi: 10.1016/j.egypro.2017.09.245.

[36] M. Pospischil *et al.*, ‘Applications of parallel dispensing in PV metallization’, in *AIP Conference Proceedings*, American Institute of Physics Inc., Sep. 2019. doi: 10.1063/1.5125870.

[37] ‘Öffentlicher Abschlussbericht des For-schungsvorhabens “Großflächige, kontaktlose Druckverfahren und Materialen zur Erzeugung feiner Struk-turen für Hocheffiziente Solarzellen” Akronym: “GECKO”’.

[38] K. Gensowski, M. Much, E. Bujnoch, S. Spahn, S. Tepner, and F. Clement, ‘Filament stretching during micro-extrusion of silver pastes enables an improved fine-line silicon solar cell metallization’, *Sci Rep*, vol. 12, no. 1, Dec. 2022, doi: 10.1038/s41598-022-16249-5.

[39] M. Pospischil *et al.*, ‘High aspect ratio front contacts by single step dispensing of metal pastes"-Rotary Printing for Si Solar Cells View project Dispensing View project HIGH ASPECT RATIO FRONT CONTACTS BY SINGLE STEP DISPENSING OF METAL PASTES’, 2010. [Online]. Available: https://www.researchgate.net/publication/216564459

[40] K. Gensowski, M. Much, E. Bujnoch, S. Spahn, S. Tepner, and F. Clement, 'Filament stretching during micro-extrusion of silver pastes enables an improved fine-line silicon solar cell metallization', *Sci Rep*, vol. 12, no. 1, Dec. 2022, doi: 10.1038/s41598-022-16249-5.

[41] K. Gensowski *et al.*, 'Dispensing of low-temperature silver pastes', in *AIP Conference Proceedings*, American Institute of Physics Inc., Jun. 2021. doi: 10.1063/5.0056103.

[42] 'ITRPV Ninth Edition Presentation 2018': http://www.pvmen.com/upload/attachment/201803/20/053037/ITRPV%20Ninth%20Edition%20Presentation%202018.pdf

[43] J. Schube *et al.*, 'FlexTrail Printing as Direct Metallization with Low Silver Consumption for Silicon Heterojunction Solar Cells: Evaluation of Solar Cell and Module Performance', *Energy Technology*, vol. 10, no. 12, Dec. 2022, doi: 10.1002/ente.202200702.

[44] D. Rudolph *et al.*, 'Screen printable, non-fire-through copper paste applied as busbar metallization for back contact solar cells', in *AIP Conference Proceedings*, American Institute of Physics Inc., Nov. 2022. doi: 10.1063/5.0127359.

[45] M. Galiazzo and N. Frasson, 'Evaluation of different approaches for HJT cells metallization based on low temperature Cu paste'.

[46] J. Yu *et al.*, 'Copper metallization of electrodes for silicon heterojunction solar cells: Process, reliability and challenges', *Solar Energy Materials and Solar Cells*, vol. 224. Elsevier B.V., Jun. 01, 2021. doi: 10.1016/j.solmat.2021.110993.

[47] Y. Zeng *et al.*, 'Review on Metallization Approaches for High-Efficiency Silicon Heterojunction Solar Cells', *Transactions of Tianjin University*, vol. 28, no. 5. Tianjin University, pp. 358–373, Oct. 01, 2022. doi: 10.1007/s12209-022-00336-9.

[48] G. Beaucarne, L. Tous, J. Lossen, and A. Faes, 'Summary of the 10thworkshop on metallization and interconnection for crystalline silicon solar cells', in *AIP Conference Proceedings*, American Institute of Physics Inc., Nov. 2022. doi: 10.1063/5.0126230.

[49] K. Chung *et al.*, 'Non-oxidized bare copper nanoparticles with surface excess electrons in air', *Nat Nanotechnol*, vol. 17, no. 3, pp. 285–291, Mar. 2022, doi: 10.1038/s41565-021-01070-4.

[50] N. Frasson and M. Galiazzo, 'Evaluation of different approaches for HJT cells metallization based on low temperature copper paste', in *AIP Conference Proceedings*, American Institute of Physics Inc., Nov. 2022. doi: 10.1063/5.0126222.

[51] B. A. Latif, 'Academic year': Master thesis

[52] K. C. Fong, K. R. McIntosh, and A. W. Blakers, 'Accurate series resistance measurement of solar cells', *Progress in Photovoltaics: Research and Applications*, vol. 21, no. 4, pp. 490–499, Jun. 2013, doi: 10.1002/pip.1216.

[53] 'The baseline for industrial production of high-efficiency silicon heterojunction solar cells'. Accessed: Jul. 15, 2023. [Online]. Available: https://www.fz-juelich.de/en/iek/iek-5/research/silicon-heterojunction-solar-cells-and-modules/the-baseline-for-industrial-production-of-high-efficiency-silicon-heterojunction-solar-cells

[54] C. L. Watts *et al.*, 'Light soaking in metal halide perovskites studied via steady-state microwave conductivity', *Commun Phys*, vol. 3, no. 1, Dec. 2020, doi: 10.1038/s42005-020-0350-2.

[55] 'TDS LF-380'.Dec2022.pdf

[56] J. Perelaer *et al.*, 'Printed electronics: The challenges involved in printing devices, interconnects, and contacts based on inorganic materials', *J Mater Chem*, vol. 20, no. 39, pp. 8446–8453, Oct. 2010, doi: 10.1039/c0jm00264j.